Journal of Physiology (1995), **489.2**, *pp.*489–510

Experimentally derived model for the locomotor pattern generator in the *Xenopus* embryo

Nicholas Dale*

School of Biological Sciences, University of Bristol, Woodland Road, Bristol BS8 1UG, UK

1. Simulations of *Xenopus* embryo spinal neurons were endowed with Hodgkin–Huxley-style models of voltage-dependent Na^+, Ca^{2+}, slow K^+ and fast K^+ currents together with a Na^+-dependent K^+ current. The parameters describing the activation, inactivation and relaxation of these currents were derived from previous voltage-clamp studies of *Xenopus* embryo spinal neurons. Each of the currents was present at realistic densities.

2. The model neurons fired repetitively in response to current injection. The Ca^{2+} current was essential for repetitive firing in response to current injection. The fast K^+ current appeared mainly to control spike width, whereas the slow K^+ current exerted a powerful influence on the repetitive firing properties of the neurons without markedly affecting spike width.

3. The properties of the model neurons could be made more consistent with those previously reported for *Xenopus* embryo neurons during intracellular recordings *in vivo*, if the shunting effect of the sharp microelectrode was incorporated into the model.

4. The model neurons were then used to create a simplified version of the spinal network that controls swimming in the frog embryo. This model network could generate the motor pattern for swimming: the activity between the left and right sides alternated with a cycle period that varied from 50 to 120 ms. This is very similar to the range of cycle periods observed in the real embryo. The shunting effect of the microelectrode was once again taken into account.

5. Reductions of the K^+ currents perturbed the motor pattern and gave three forms of aberrant motor activity very similar to those previously seen during the application of K^+ channel blockers to the real embryo. The ability to generate the correct motor pattern for swimming in the model depended on the balance between the K^+ currents and the inward Na^+ and Ca^{2+} currents rather than their absolute values.

6. The model network could generate a motor pattern for swimming over a very wide range of excitatory (2–10 nS) and inhibitory (2–400 nS) synaptic strengths. Rough estimates of the physiological synaptic strengths in the real circuit (around 20–60 nS for inhibition and 2–5 nS for excitation) fall within the range of synaptic strengths that gave simulation of the swimming motor pattern in the model.

7. The cycle period of the motor activity in the model shortened either as the excitatory synapses were strengthened or as the inhibitory synapses were weakened.

8. The prediction that the strength of the mid-cycle inhibition determines cycle period has been tested by using low levels of strychnine to reduce glycinergic reciprocal inhibition in a graded manner in the real embryo. As the inhibition was reduced, the cycle period of fictive swimming in the embryo shortened by amounts very close to those predicted by the model.

9. This new experimentally derived model can replicate many of the known features of fictive swimming in the real embryo and may be of value as an analytical tool in attempting to understand how the spinal circuitry of the *Xenopus* embryo and related amphibian embryos control a variety of motor behaviours.

* Present address: School of Biological and Medical Sciences, Bute Medical Building, University of St Andrews, St Andrews, Fife KY16 9TS, UK.

The operation of a neural circuit is determined not only by the way the component neurons are connected but also by the properties of its component neurons and synapses (e.g. Dickinson, 1989; Soffe, 1991). Thus a complete description of the mechanisms underlying the operation of a neural circuit would include: (1) the elucidation of the underlying wiring diagram; (2) the characterization of the kinetics of the voltage-gated currents; and (3) identification of the transmitters and receptors involved together with the kinetics of their synaptic potentials (Selverston, 1980). Once this has been achieved, the contribution of the properties of the various ionic currents and synaptic potentials to the determination of neuronal properties and the operation of the circuit has to be understood. Two approaches to solve this problem are presently available. First, pharmacological agents could be used to manipulate the individual components in a selective manner while studying their effects on neuronal properties and circuit function (e.g. Hill, Matsushima, Schotland & Grillner, 1992; Tierney & Harris-Warrick, 1992; Wall & Dale, 1994*a*, 1995). Second, physiologically based computer models can be created, which incorporate accurate descriptions of the known components and thus give understanding of how they may contribute to circuit function (e.g. Getting, 1989; Traub, Wong, Miles & Michelson, 1991; McCormick & Huguenard, 1992). Since pharmacological agents often have poor specificity, they may affect several components of the circuit at the same time and thus lead to difficulties in interpreting the role of any single component in contributing to neuronal properties and circuit function. In a computer model, the individual components can be modified in highly specific ways, which potentially allows very fundamental understanding of how, for example, ion channels contribute to circuit function. However, a computer model is only as good as the information from which it is created and it can only be thought of as a hypothesis, which should be subject to experimental testing.

The *Xenopus* embryo is a model for studying the control of locomotion in vertebrates and has several advantages for this study. It has an extremely simple nervous system: the spinal cord has only eight anatomical classes of neuron at this stage (Roberts & Clarke, 1982). Furthermore, the neurons have very limited dendritic arborizations (Roberts & Clarke, 1982), allowing the neurons to be modelled as a single compartment. The neural circuit and transmitters underlying the control of swimming have been elucidated (Dale, 1985; Dale & Roberts, 1985; Arshavsky, Orlovsky, Panchin, Roberts & Soffe, 1993; Perrins & Roberts, 1995*a*, *b*). Computer simulations of this neural circuit have been attempted (Roberts & Tunstall, 1990; Wall & Dale, 1994*a*; Wolf & Roberts, 1995; Roberts, Tunstall & Wolf, 1995). However, these previous simulations have not been able to incorporate data from voltage-clamp studies of *Xenopus* neurons. More realistic simulations that include the voltage-gated ion channels present in *Xenopus* spinal neurons are thus required to allow a better understanding of how the spinal circuitry generates the motor pattern for swimming.

In the accompanying paper (Dale, 1995) I have characterized the ionic currents possessed by *Xenopus* spinal neurons and created Hodgkin–Huxley-style kinetic models to describe them. In this paper, these models of the individual currents have then been incorporated into simulations of both single neurons and networks of neurons. I have been able to conclude that a combination of the known circuitry together with the ionic currents that I have described is *sufficient* to generate a motor pattern remarkably similar to swimming in the real animal. This new simulation suggests that the circuit functions in a manner rather different from that proposed in previous modelling studies and gives rise to several predictions. I have experimentally tested one of these: the possibility that the magnitude of the reciprocal inhibition is an important determinant of the swimming cycle period.

METHODS

Simulation program

The simulation program ran on an IBM-compatible PC (under the protected mode to give 32 bit memory addressing) and was written in an object-oriented language, C++ (Symantec). The neurons were simulated by a single compartment model and the well-known principal equation for specifying how the transmembrane voltage of each neuron varied with time was given by:

$$C_{\mathrm{m}}\frac{\mathrm{d}V}{\mathrm{d}t} = -(I_{\mathrm{inj}} + I_{\mathrm{Na}} + I_{\mathrm{Ca}} + I_{\mathrm{K}_f} + I_{\mathrm{K}_s} + I_{\mathrm{K_{Na}}} + I_{\mathrm{leak}} + I_{\mathrm{syn}}), \quad (1)$$

where C_{m} is the cell's capacitance, I_{inj} the injected current, and I_{Na}, I_{Ca}, I_{K_f}, I_{K_s}, $I_{\mathrm{K_{Na}}}$, I_{leak} and I_{syn} represent the Na^+, Ca^{2+}, fast K^+, slow K^+, Na^+-dependent K^+, leak and synaptic currents, respectively. The Na^+, Ca^{2+} and voltage-gated K^+ currents were implemented in this simulation study by the equations given in the accompanying paper (Dale, 1995), while the Na^+-dependent K^+ current and the control of submembrane Na^+ were implemented by the equations given in Dale (1993).

$$I_{\mathrm{leak}} = g_{\mathrm{leak}}(V - E_{\mathrm{rev}}), \quad (2)$$

where E_{rev} was the reversal potential for the leak current and was set to give the simulated neurons a resting potential of −70 mV. The input conductance, g_{leak}, was set to 1 nS, a value typical of the isolated neurons (Dale, 1991).

Model of synaptic transmission. Synaptic transmission was modelled by a threshold detection method. When a voltage threshold in the presynaptic neuron had been crossed (0 mV) and $\mathrm{d}V/\mathrm{d}t$ had exceeded 0·1 mV ms^{-1} a synaptic current was evoked in the postsynaptic neuron following an adjustable delay that represented a combination of the conduction time down the axon of an impulse and the synaptic delay. The synaptic currents (I_{syn}) were modelled by:

$$I_{\mathrm{syn}} = g_{\mathrm{syn}}(1 - \mathrm{e}^{-t/\tau_{\mathrm{o}}})\mathrm{e}^{-t/\tau_{\mathrm{c}}}(V - E_{\mathrm{rev}}), \quad (3)$$

where g_{syn} is the maximal amplitude of the synaptic conductance, t the time after the start of the synaptic current, τ_{o} and τ_{c} are the opening and closing rate constants, respectively, and E_{rev} is the reversal potential for the synaptic current. Synaptic currents evoked by a single synapse were allowed to summate temporally.

However, given that transmitter release from a single quantum may almost saturate the postsynaptic receptor plaque (e.g. Korn, Triller, Mallet & Faber, 1981; Redman & Walmsley, 1983), it seems likely that the strength of a single synaptic contact will saturate at some value and not summate *ad infinitum*. The maximal summated conductance at a single synapse was therefore arbitrarily set to be 20% greater than g_{syn}. Thus:

$$g_{sum} = g_{syn} \sum_{i=1}^{n} (1 - e^{-t_i/\tau_o}) e^{-t_i/\tau_c} \qquad (g_{sum} \leqslant 1{\cdot}2\, g_{syn}), \qquad (4)$$

where g_{sum} is the temporally summated conductance and t_i is the time after the start of the ith synaptic potential. This feature of saturation during summation was not critical to the results of the simulations, which gave similar results if $g_{sum} = g_{syn}$ or if no limit was placed on g_{sum}. Equation (3) thus became:

$$I_{syn} = g_{sum}(V - E_{rev}). \qquad (5)$$

At some point, to save computational effort, a synaptic current has to be deemed to be finished and thus removed from the temporal summation in eqn (4). Thus when:

$$e^{-t_i/\tau_c} \leqslant lim, \qquad (6)$$

the synaptic current was considered to be essentially complete. By experimenting with various values, *lim* was set to be 0·001. This gave fast simulation times without altering the result of the simulation.

The parameters used to specify the kinetics of the synaptic currents (τ_o and τ_c) were taken from values published in the literature: for the non-NMDA receptor-mediated and glycine receptor-mediated synaptic currents τ_o was set at 0·5 ms and τ_c at 4 and 6·5 ms (Forsythe & Westbrook, 1988; Korn & Faber, 1990), respectively; while for the NMDA receptor-mediated synaptic currents τ_o and τ_c were respectively set to 5 and 80 ms (Forsythe & Westbrook, 1988). The magnitude of the conductance underlying the non-NMDA receptor-mediated EPSCs was made to be always twice that underlying those mediated by the NMDA receptor.

Numerical integration was performed by a 4th order Runge–Kutta algorithm with adaptive step size (Press, Flannery, Teukolsky & Vetterling, 1988).

Channel densities in modelled neurons. To simulate single neurons, it was necessary not only to model the ionic currents but also to endow the modelled neurons with the channels at densities similar to those observed in real embryonic neurons. The maximal conductances, or in the case of the K^+ and Ca^{2+} currents the maximal permeability to K^+ and Ca^{2+}, were measured from the data presented by Dale (1995) and divided by the neuron's capacitance to give a specific conductance or permeability (essentially a measure of the number of channels per unit of membrane area; Table 1). The model neurons were then given channel densities within this observed range. The mean values are likely to underestimate the magnitude of the conductances in intact real neurons for two reasons: (1) the acutely isolated neurons lose a substantial proportion of their dendrites and axon; and (2) some currents, such as Ca^{2+} currents, are subject to run-down. To compensate at least partly for this, the model neurons were given channel densities at the high end of the observed range.

Physiological experiments

Recording from isolated neurons. Acutely isolated neurons were obtained using the methods described in the preceding paper. Whole-cell patch clamp recordings were made (see Dale, 1995) to study the response of the neurons to 100 μM glycine and the antagonistic action of strychnine. These drugs were applied rapidly through a multibarreled microperfusion system (Dale, 1995).

Electrophysiological recordings from whole embryos. These experiments were performed in accordance with the UK Animals (Scientific Procedures) Act, 1986. To facilitate handling, stage 37/38 *Xenopus* embryos (Nieuwkoop & Faber, 1956) were anaesthetized in tricaine methanesulphonate (MS222; Sigma) and their dorsal fins slit using fine pins. They were then allowed to recover from the anaesthetic before being treated with the neuromuscular blocking agent α-bungarotoxin (at 0·077 mg ml^{-1}). The paralysed embryos were then prepared for extracellular ventral root recordings using the methods described by Kahn & Roberts (1982). The spinal cord was transected at the level of the first postotic myotome, and electrical stimuli to the skin were used to trigger swimming episodes. The cycle period of swimming was measured on-line, using an electronic device that rectified the ventral root burst, converted it to a transistor–transistor logic pulse, and measured the time interval between consecutive ventral root bursts.

Strychnine was bath applied at concentrations from 1 to 100 nM. The bath volume was very small (about 0·5 ml) and thus allowed fast change-over of solutions. To facilitate access of strychnine to the nervous system, rostral myotomes were removed from each side of the spinal cord and the dorsal attachment of the remaining myotomes on both sides was loosened with fine pins.

Table 1. Maximal conductance and permeability values for the currents observed in isolated *Xenopus* embryo neurons during whole-cell patch clamp recordings and the 'control' values given to the model neurons

Channel	I_{Na} (nS pF^{-1})	I_{Ca} (cm s^{-1} pF^{-1} × 10^9)	I_{K_f} (cm s^{-1} pF^{-1} × 10^9)	I_{K_s} (cm s^{-1} pF^{-1} × 10^9)	$I_{K_{Na}}$ (nS pF^{-1})
Conductance and permeability ranges for isolated neurons					
Magnitude (range)	8·3–37·1[a]	0·02–0·22[a]	0·025–0·054[a]	0·011–0·022[a b]	2–5[c]
Mean ± S.E.M. (n)	19 ± 5·3 (5)[a]	0·078 ± 0·018 (9)[a]	0·038 ± 0·004 (8)[a]	0·015 ± 0·002 (4)[a b]	—
Conductance and permeability values for model neurons					
Magnitude	30	0·15	0·05	0·02	5

All conductance and permeability measurements are normalized to the input capacitance of neurons. [a]Based on data presented by Dale (1995). [b]Assuming a mean cell capacitance of 9·5 ± 0·39 pF (n = 24). [c]From Dale (1993) assuming 33% of total outward current is the Na^+-dependent K^+ current and a mean cell capacitance of 9·5 pF.

RESULTS

Computer simulations of single neurons

Membrane properties. By removing the Na^+ current from the model neurons (simulating the action of TTX) strong membrane rectification could be revealed. When depolarizing current was injected into the model neurons, the membrane responded in a non-linear fashion and was resistant to depolarization much above −40 mV (Fig. 1*A*). This is quite similar to the membrane rectification reported for *Xenopus* spinal neurons recorded *in vivo* with sharp microelectrodes (cf. Fig. 6*C* of Soffe, 1990) and for acutely isolated *Xenopus* neurons (cf. Fig. 7 of Dale, 1991).

When both the Na^+ and Ca^{2+} currents were present, the model neurons responded to current injection by firing a train of spikes, the frequency of which graded with the amount of current injected (Fig. 1*B*). The Ca^{2+} current appeared important for allowing repetitive firing: if it was removed, the neurons became capable of firing only one action potential (Fig. 1*C*). Repetitive firing could be evoked in the absence of a Ca^{2+} current, but only by increasing the Na^+ current to a value outside the range observed in the isolated neurons. Experimental evidence supports the notion that the Ca^{2+} current is important for spike initiation: ω-conotoxin, which blocks roughly half the Ca^{2+} current, raises spike thresholds in *Xenopus* motoneurons (Wall & Dale, 1994*b*).

Effect of voltage-gated K^+ currents on repetitive firing. Previous experimental evidence obtained both from neurons *in vivo* and acutely isolated neurons suggests that voltage-gated K^+ currents play a role in determining the firing properties of *Xenopus* spinal neurons (Soffe, 1990; Dale, 1991). To test the contribution of the fast and slow K^+ currents to the control of repetitive firing, their amplitudes in the modelled neurons were systematically varied.

As the fast current was reduced from its 'control' value, the spike threshold was lowered (Fig. 2*A a*) and the spike width increased (Fig. 2*A b*). However, reducing the fast current was ineffective in allowing the neuron to fire at higher frequencies (Fig. 2*A*). By contrast, reductions in the slow current had little effect on spike width (Fig. 2*B b*), gave a lesser reduction in spike thresholds but dramatically altered the repetitive firing properties of the model neurons (Fig. 2*B a*). Thus the fast and slow K^+ currents appear to subserve different roles, the former being mainly responsible for action potential repolarization, while the latter exerts powerful control over the repetitive firing properties of the model neurons.

Effect of input resistance on membrane properties. Previous reports based upon extensive intracellular recordings from *Xenopus* spinal cord neurons *in vivo* suggest that they are rarely capable of firing repetitive

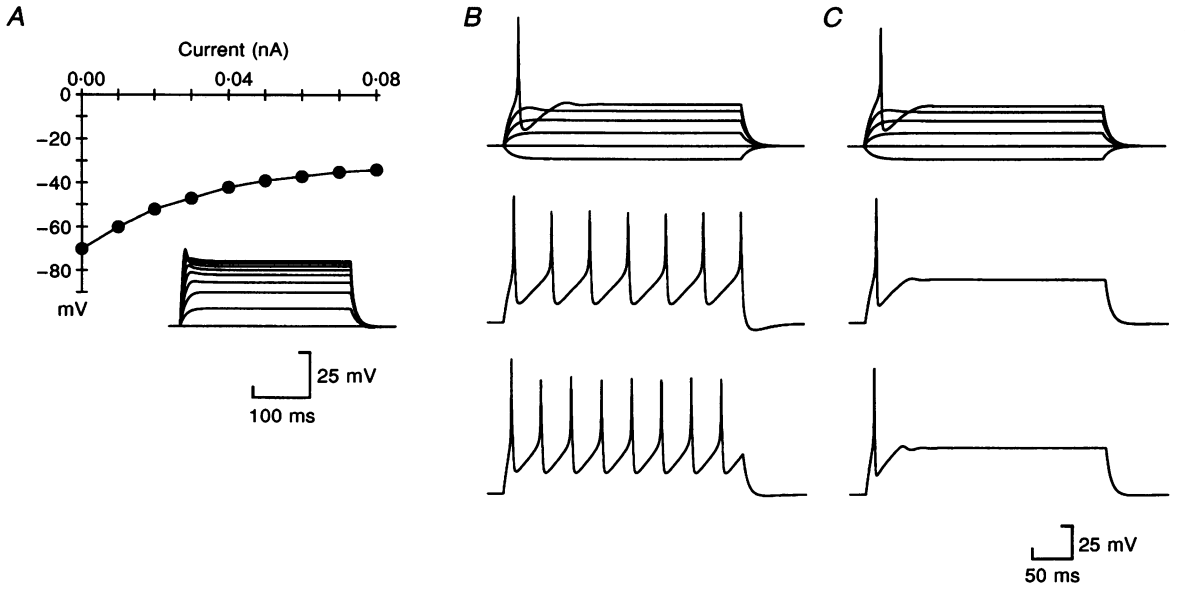

Figure 1. Membrane properties of the model neurons

A, in the absence of the Na^+ current, strong membrane rectification can be revealed. Inset shows responses to pulses of depolarizing current from 0 to 0·08 nA. *B*, the model neurons fire repetitively in response to current injection. Response to: current pulses from −0·01 to 0·04 nA in 0·01 nA steps (top), current pulse of 0·05 nA (middle) and 0·06 nA (bottom). *C*, when the Ca^{2+} current was absent repetitive firing in the model neurons was not seen. The top, middle and bottom portions of *C* are exactly equivalent to those in *B*.

trains of action potentials in response to current injection (Soffe, 1990). In contrast, the model neurons readily fired non-accommodating trains of spikes in a manner apparently inconsistent with these previously described properties. However, the modelled neurons were given an input resistance of 1 GΩ based upon the values obtained from acutely isolated neurons (Dale, 1991). During intracellular recording, *Xenopus* neurons have a mean input resistance of around 100 MΩ. This much lower value presumably results from the damage introduced by the sharp microelectrode. To test whether this shunt could account for the differences between the properties of the model neurons and those recorded *in vivo*, the input resistance of the modelled neurons was shunted to 200 MΩ (equivalent to a 'good' intracellular recording).

The shunted neurons now fired only a single action potential in response to current injection that was followed by a relatively small and short after-hyperpolarization (AHP; Fig. 3*A*). This behaviour was very similar to that reported for neurons during intracellular recordings (cf. Figs 1, 3, 5 and 6 of Soffe, 1990). However, one difference between the shunted model neurons and their real counterparts was that during large amounts of current injection small oscillations of membrane potential were seen (Fig. 3*A*, bottom trace). This behaviour has not been reported in real neurons, disappeared as more current was injected and could be removed from the modelled neurons by reducing the Ca^{2+} current slightly (by 30%).

Injection of Cs^+ ions into neurons in the spinal cord can make them fire repetitively (Soffe, 1990). It was therefore

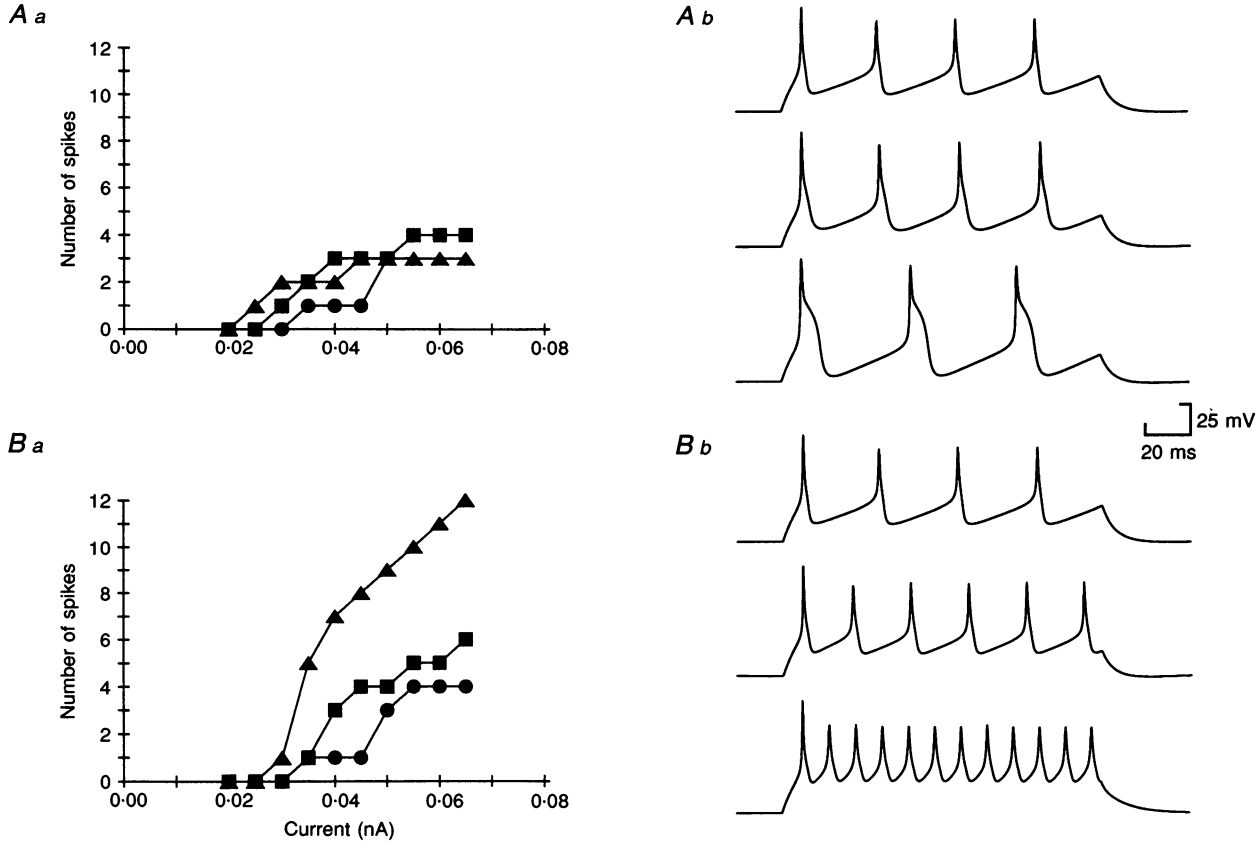

Figure 2. The role of K^+ channels in controlling spike width and membrane excitability

A a, although the fast K^+ current contributes little to the control of repetitive firing, it does help to set the firing threshold. ●, fast K^+ current present at control value; ■, halved in amplitude; and ▲, completely absent. *A b*, the fast current repolarizes the action potential: as the K^+ current is reduced from the control (top trace) to half-amplitude (middle trace) and to zero (bottom trace) the spikes become broader. *B a*, the slow K^+ current contributes to membrane threshold and has a dramatic effect on the repetitive firing properties of the model neurons. ●, control; ■, slow K^+ current halved; and ▲, completely absent. *B b*, the slow K^+ current has little effect on spike width. Top trace, control; middle trace, slow K^+ current halved; bottom trace, slow K^+ current absent. The records in *A b* and *B b* show responses during injection of 0·065 nA of current.

important to see whether the shunted model neurons could also be persuaded to fire repetitively by reducing their K^+ currents. In contrast to the non-shunted neurons, it now appeared that reductions of the fast K^+ current were most effective at promoting repetitive firing. Reducing the slow current by 50% gave only small repetitive spikelets (Fig. 3*B*), whereas an equivalent reduction in the fast current gave trains of much bigger and faster spikes (Fig. 3*C*). In the model neurons, the first spike of the train was always substantially bigger than those following. This is presumably due to an increased level of Na^+ channel inactivation following the first spike and suggests that the AHP in the shunted model neurons is insufficient to completely remove this inactivation. In real neurons the spikes tend to stay the same amplitude throughout the train (e.g. Fig. 8 of Soffe, 1990).

Thus the properties of the model neurons can be made much more consistent with those described in spinal cord neurons during intracellular recording if the membrane shunt introduced by the sharp microelectrode is taken into account. Minor differences between the shunted model neurons and real neurons nevertheless remain.

Simulation of the locomotor network

The known circuitry underlying the control of swimming in the *Xenopus* embryo (Dale, 1985; Dale & Roberts, 1985; Perrins & Roberts, 1995*a*,*b*; Fig. 4*A*) was condensed and simplified to a two-cell net that consisted of two self-exciting neurons that could reciprocally inhibit each other (Fig. 4*B*). Similar simplifications of the locomotor circuit were used by Roberts & Tunstall (1990). Motor activity in the circuit was triggered by 'sensory' synapses, which mimicked the inputs to the spinal cord from the Rohon–Beard neurons (Clarke & Roberts, 1984; Roberts & Sillar, 1990). These synaptic currents had a τ_0 of 0·5 ms and a τ_c of 80 ms, mimicking the NMDA receptor-mediated and non-NMDA receptor-mediated excitation known to occur in this sensory pathway (Roberts & Sillar, 1990; Sillar & Roberts, 1992). A single sensory EPSC was given to both the left and right neurons (with conductances of 3 and 2 nS, respectively). The right neuron was stimulated 30 ms before the left (cf. Roberts & Tunstall, 1990; Sillar & Roberts, 1992).

The model was able to replicate the motor pattern for swimming over a wide range of synaptic strengths (Figs 5 and 11). The output from the circuit consisted of alternating discharge of the two neurons, each firing a single spike. The cycle periods of this activity ranged from 50 to 120 ms depending upon the amplitude of the synaptic connections (see later). This is very similar to the range of cycle periods reported in the real embryo (Kahn & Roberts,

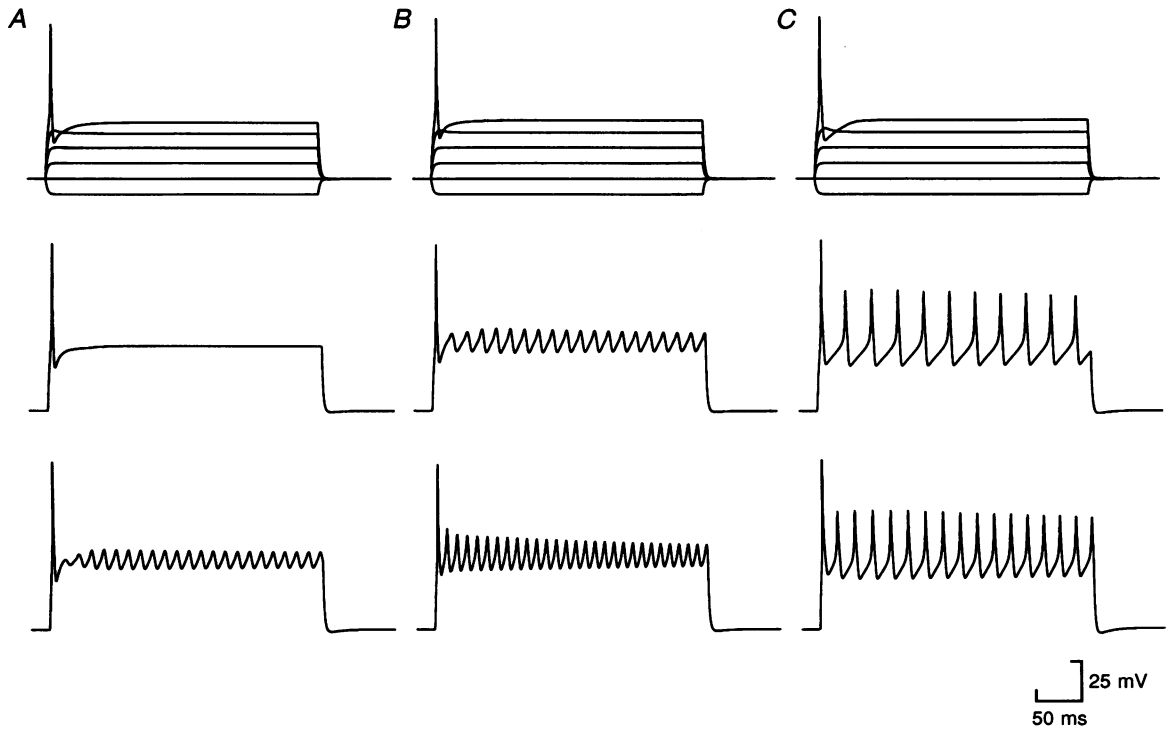

Figure 3. Simulation of membrane shunting by intracellular microelectrode reduces membrane excitability

A, responses of control cell shunted to 200 MΩ. Responses of shunted neurons to current injection when slow K^+ current halved (*B*) and fast K^+ current halved (*C*). In all 3 parts of the figure top traces show responses to −0·1 to 0·4 nA, middle traces to 0·5 nA and bottom traces to 0·6 nA.

1982; Soffe & Roberts, 1989) and suggests that the mechanisms incorporated into this simplified network model are sufficient to explain at least some aspects of motor pattern generation.

Despite the similarity of the overall motor pattern, there were some significant differences between the details of the pattern seen in the model and that in the real embryo. First, the mid-cycle level of membrane potential in the real embryo measured just before the IPSP is usually around −40 to −50 mV. Yet in the modelled neurons this was significantly more positive, around −33 mV (Fig. 5). Neurons in the real embryo rarely show much evidence of an AHP during swimming (Dale & Roberts, 1984, 1985; Soffe, Clarke & Roberts, 1984; Soffe, 1987, 1993). However, in the modelled neurons the spikes were followed by a series of after-potentials (Fig. 5).

To investigate whether these discrepancies could be explained by the membrane shunting caused by intracellular recording, I introduced a third slave cell to the circuit. The slave cell had properties identical to those of the other two neurons except that its membrane resistance was now only 200 MΩ. Since the slave cell only received inputs from the other two cells and did not otherwise participate in the circuit, it was merely a device to monitor the shunting effect of the microelectrode without altering activity in the two-cell network. The membrane shunting in the slave neuron completely eliminated the spike after-potentials and lowered the mid-cycle membrane potential to around −50 mV (Fig. 5). It also revealed depolarizing prepotentials underlying the spike and changed the shape of the falling phase of the mid-cycle IPSPs (Fig. 5). This shape of mid-cycle IPSP and the prepotentials are common features seen during intracellular recordings from many spinal neurons (e.g. Roberts & Kahn, 1982; Soffe & Roberts, 1982; Soffe, Clarke & Roberts, 1984; Dale, 1985). Once again, the modelling suggests that damage caused by intracellular recording may significantly alter the observed pattern of activity from that which occurs in the undamaged neurons.

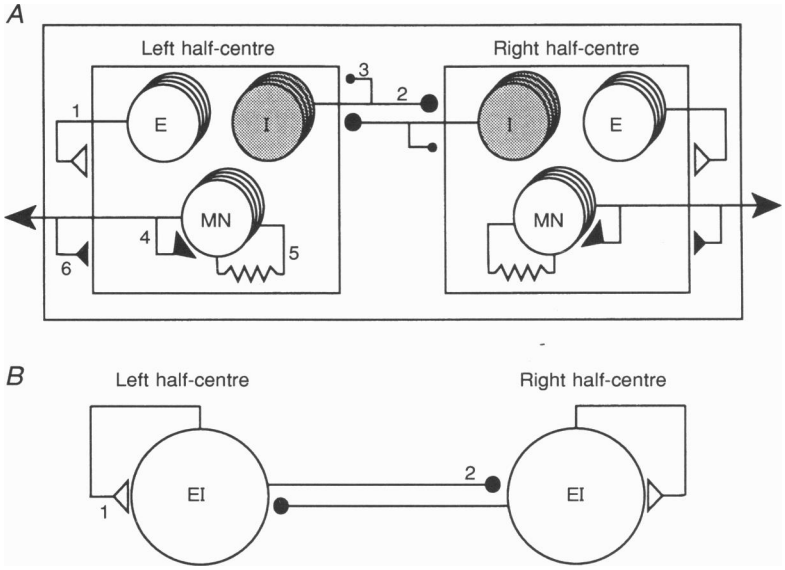

Figure 4. The spinal circuitry underlying the control of swimming in the *Xenopus* embryo

A, connections thought to exist within the spinal circuitry (diagram based on Perrins & Roberts, 1995*b*) between the excitatory interneurons (E), inhibitory interneurons (I) and motoneurons (MN). The circles represent populations of about 150 excitatory, 300 inhibitory and 300 motor neurons on each side of the spinal cord. (1) Feedback excitation from the excitatory interneurons, mediated by an excitatory amino acid receptor at NMDA and non-NMDA synapses, to all neurons within the half-centre (Dale & Roberts, 1985). (2) Reciprocal inhibition mediated by the glycinergic interneurons onto every member of the opposite half-centre (Dale, 1985). (3) Weak recurrent inhibition also mediated by glycine receptors to all neurons of the half-centre (Dale, 1985). (4) Cholinergic excitation between motoneurons mediated by nicotinic receptors (Perrins & Roberts, 1995*a*). (5) Electrical coupling between motoneurons (Perrins & Roberts, 1995*a*). (6) Cholinergic excitatory connections made from motoneurons to the premotor interneurons via nicotinic receptors (Perrins & Roberts, 1995*b*). *B*, the simplified version of this circuitry used for the computer simulations. The populations of excitatory and inhibitory interneurons have been combined into one type of dual-function neuron (EI) that can excite themselves via NMDA and non-NMDA receptors (1) and inhibit each other (2). In all simulations the non-NMDA component of excitation was twice that mediated by the NMDA receptors.

Effect of voltage-gated K^+ currents on motor pattern generation. The K^+ currents have an important role in stabilizing motor pattern generation in the real embryo. Even small reductions of 15–30% in the total outward currents can severely disrupt motor pattern generation (Wall & Dale, 1994*a*). I therefore systematically studied the possible roles of the K^+ currents in the model. Reducing the fast K^+ current by half caused slight abnormalities at the beginning of the activity in the model (Fig. 6*A*), which were very reminiscent of the 'type A' pattern seen during application of non-specific K^+ channel blockers to the real embryo (cf. Figs 6–8 of Wall & Dale, 1994*a*). Reduction of the slow K^+ current by half caused extra spikelets to be evoked immediately following the main spike, but did not otherwise disrupt the motor pattern (Fig. 6*B*). Abnormalities of this sort have not been seen during applications of K^+ channel blockers to the real embryo (Wall & Dale, 1994*a*). If both the fast and the slow K^+ currents were reduced by half, much greater disruptions of the motor pattern resulted (Fig. 6*C*). The neurons showed all three types of abnormality seen during applications of K^+ channel blockers to the real embryo (compare Fig. 6 with Figs 6–8 of Wall & Dale, 1994*a*). If the slow K^+ current was completely removed, motor pattern generation was completely disrupted (Fig. 9*A*), suggesting that this current is essential for operation of the model. By contrast, motor pattern generation survived complete elimination of the fast K^+ current.

In a previous study, the balance between the inward and outward currents of spinal neurons rather than their absolute magnitudes was proposed to be crucial for motor pattern generation (Wall & Dale, 1994*a*). To test whether this was true for the model, I reduced all K^+ currents by half. This resulted in severe disruption at the beginning of the motor pattern (Fig. 7*A*). However, if the Na^+ and Ca^{2+} currents were subsequently reduced by a third, normal motor pattern generation was restored (Fig. 7*B*). This supports the proposal that it is the net balance of the currents that determines whether correct pattern generation occurs rather than their absolute magnitudes.

Possible roles for Na^+-dependent K^+ current. *Xenopus* spinal neurons posses a Na^+-dependent K^+ current (Dale, 1993). Previous studies have suggested that this Na^+-dependent K^+ current could play a feedback role and serve to correct the balance between the inward and outward currents on a cycle-by-cycle basis (Dale, 1993; Wall & Dale, 1994*a*). Neural activity was proposed to lead to the accumulation of submembrane Na^+ and hence greater activation of the Na^+-dependent K^+ current. The simulation studies here confirm earlier crude predictions (Dale, 1993) that Na^+ builds up over the first 1–2 s at the start of a swimming episode (Figs 5–8).

I have investigated the possible roles of the Na^+-dependent K^+ current. First, it may contribute to spike repolarization. By reducing the voltage-gated K^+ currents by half and

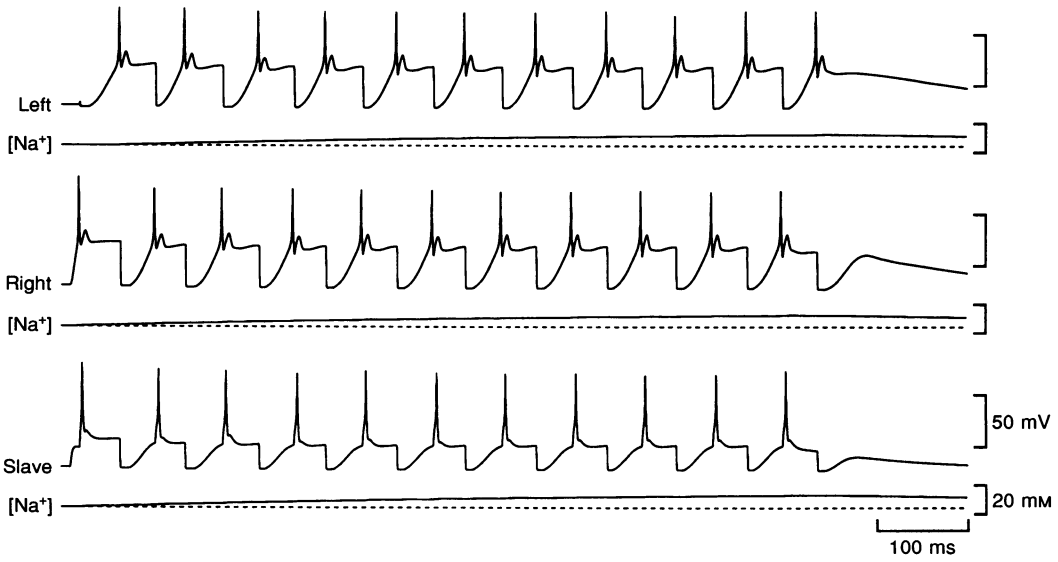

Figure 5. Simulation of a 2-cell circuit can reproduce the pattern for swimming

Discharge in the left and right neurons alternates. Submembrane Na^+ builds up throughout the activity. The slave neuron had an input resistance of 200 MΩ and received excitatory and inhibitory drive from the left and right neurons, respectively. The pattern of activity in the slave neuron was very similar to that seen during intracellular recording from spinal neurons. The inhibitory conductance was 50 nS, while the non-NMDA and NMDA receptor-mediated excitatory conductances were 4 nS and 2 nS, respectively. The tops of the voltage and $[Na^+]$ scale bars represent 0 mV and 20 mM Na^+, respectively, in this and all subsequent figures.

setting submembrane Na^+ to 5 mM, I broadened the spike (Fig. 8*A*). I then increased the submembrane Na^+ to 10 mM, thus increasing the Na^+-dependent K^+ current. This narrowed the spikes and slightly increased the excitability of the neuron (presumably by speeding up repolarization of the action potential). Thus the Na^+-dependent K^+ current can contribute to action potential repolarization and the control of membrane excitability.

To test whether the Na^+-dependent K^+ current could compensate for abnormalities occurring during motor pattern generation, I reduced the slow voltage-gated K^+ current to zero. In the virtual absence of the Na^+-dependent K^+ current the model produced a prolonged burst of spikes in only one of the neurons (Fig. 9*A*). When the Na^+-dependent K^+ current was set to its control value (Table 1), the build-up of the current moderated the burst of spikes but was unable to restore motor pattern generation (Fig. 9*B*). However, if the amplitude of the Na^+-dependent K^+ current was set at double the control value the build-up of submembrane Na^+ and the Na^+-dependent current was sufficient to restore alternating motor pattern generation (Fig. 9*C*). The Na^+-dependent K^+ current can

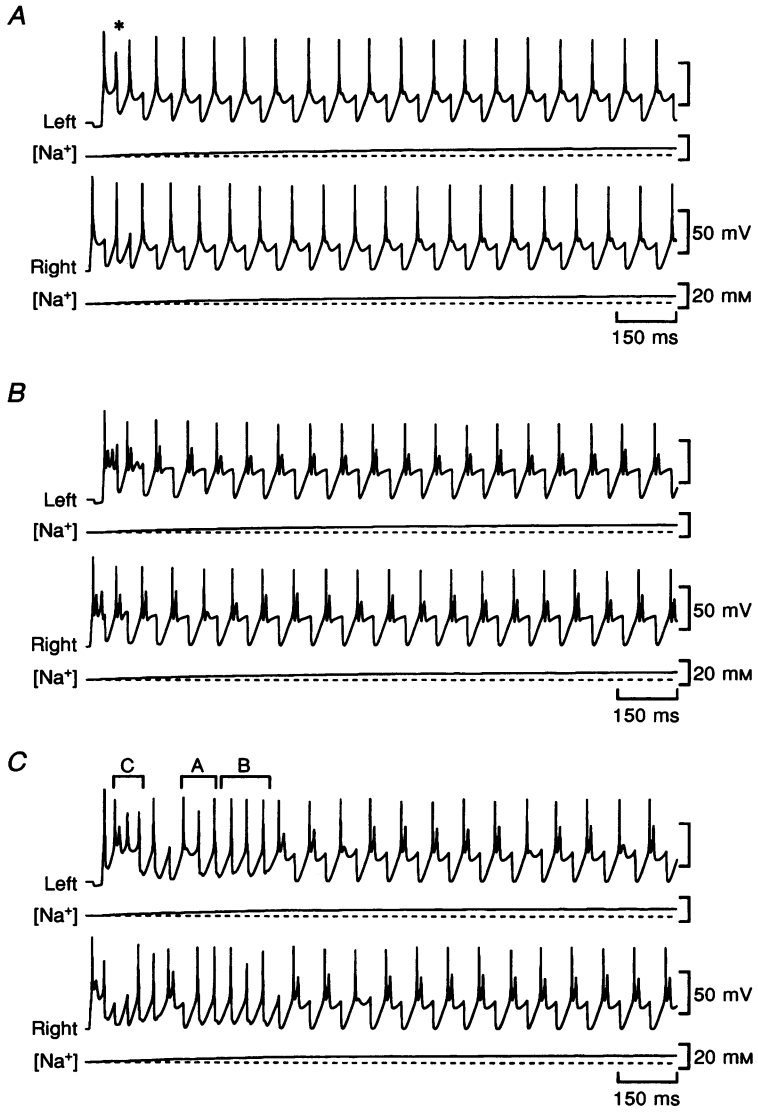

Figure 6. The role of K^+ currents in stabilizing motor pattern generation in the 2-cell circuit

A, simulation in which the fast K^+ current was halved from control value. One cycle of type A activity is seen at the beginning of the simulation (*), followed by normal alternating activity. *B*, activity after the slow K^+ current was halved was almost normal. Small spikelets are seen following the main action potential. *C*, when both the slow and fast K^+ currents were reduced, substantial abnormalities, including activity of types A, B and C, occurred at the beginning of the motor activity (shown by bars). The inhibitory conductance was 10 nS, while the non-NMDA receptor-mediated and NMDA receptor-mediated excitatory conductances were 2 nS and 1 nS, respectively.

therefore compensate for abnormalities in pattern generation, but only if increased above the control levels given in Table 1. A better description of the properties of the Na^+-dependent K^+ current and its magnitude in spinal neurons may be required so that its role can be more accurately assessed.

Introduction of recurrent inhibition in the circuit. A small but poorly defined proportion of inhibitory interneurons make recurrent connections in addition to their main reciprocal inhibitory connections (Dale, 1985; Roberts, Dale, Ottersen & Storm-Mathisen, 1988). The levels of recurrent inhibition within the circuit are very much lower than those of the reciprocal inhibition and the recurrent inhibition is only a minor component of the total synaptic drive (Dale, 1985; Tunstall & Roberts, 1994). Despite this, the recurrent inhibitory connections may have some influence over the operation of the neural circuit once the reciprocal connections have been severed (Soffe, 1989). I therefore introduced recurrent inhibitory connections into the circuit. At low levels of recurrent inhibition (< 3 nS) the pattern of activity generated in this new circuit was very similar to that already obtained in the absence of recurrent inhibition (Fig. 10*A*). However, at greater levels of recurrent inhibition it became very difficult to obtain alternating activity from the model: the left and right neurons tended to fire simultaneously, or one neuron would fire and continually inhibit the other (cf. Roberts & Tunstall, 1990). This suggests that better information is needed about the strength of recurrent inhibition.

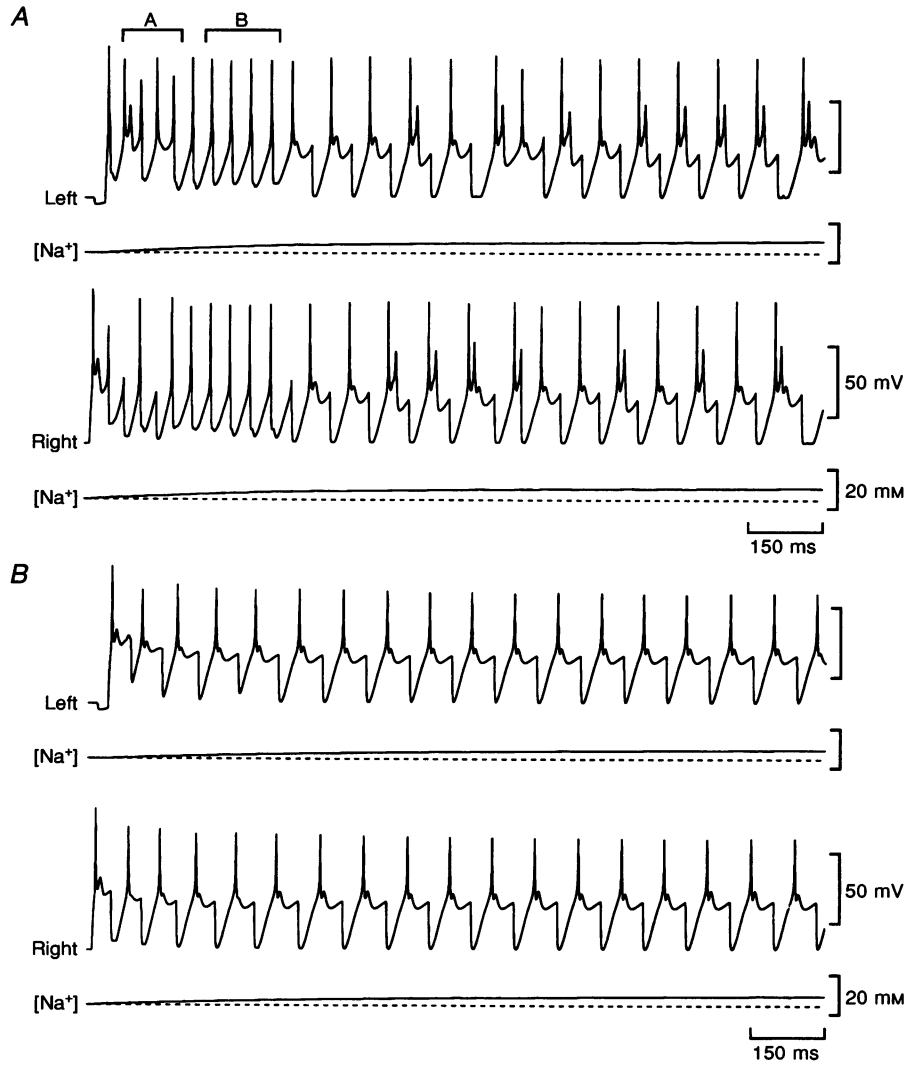

Figure 7. The balance between inward and outward currents is critical for the correct motor pattern generation

A, all K^+ currents were halved in amplitude to disrupt motor pattern generation. Type A and type B activity (shown by bars) occurred at the beginning of the activity. *B*, when the Na^+ and Ca^{2+} currents were also reduced (by 33%) normal alternating activity resumed. The inhibitory conductance was 10 nS, while the non-NMDA receptor-mediated and NMDA receptor-mediated excitatory conductances were 2 nS and 1 nS, respectively.

Following the introduction of small levels of recurrent inhibition, the circuit became much more sensitive to alterations in the level of K^+ currents. A reduction of both the slow and fast K^+ currents by 25% (ineffective at disrupting the motor pattern in the absence of recurrent inhibition) gave all three types of aberrant activity described previously (Fig. 10*B*; Wall & Dale, 1994*b*). Introduction of recurrent inhibition may therefore make the circuit slightly more realistic. However, since this component of the synaptic drive in the locomotor circuit is poorly characterized and is clearly not essential for operation of the model I have omitted it in all subsequent simulations.

The strength of synaptic drive. In the real embryo, the strength of synaptic connections within the spinal circuitry has not been directly measured. However, it is possible to make some estimates of the strength of the synaptic drive based on information in the literature. If the size of a single quantum for the EPSPs and IPSPs is around 2–6 mV (Dale, 1985; Dale & Roberts, 1985; Wall & Dale, 1993), the inhibitory reversal potential approximately −75 mV, the excitatory reversal potential 0 mV and the neuronal input resistance (under which these measurements were obtained) around 100 MΩ, then the conductance of a single inhibitory and excitatory quantum would be around 4–12 nS and 0·3–0·9 nS, respectively. Thus to obtain the conductance of the total inhibitory and excitatory drive some estimate of the quantal content of the IPSPs and EPSPs during swimming is needed. This has been measured for inhibition and is roughly 5 (Wall & Dale, 1993). Thus if both the inhibitory and excitatory drive are given roughly same quantal contents then the total conductances are around 20–60 nS and 2–5 nS, respectively. While these very rough calculations give guides as to plausible magnitudes for the synaptic conductances within the circuit, these estimates could be wrong by at least a factor of 2.

A systematic study was made of how varying synaptic strength altered the activity generated by the model. The model could continue to generate a motor pattern similar to that of swimming as the excitatory conductance was varied from 2 to 10 nS (Fig. 11*A*). This range encompasses the estimates for the level excitation in the real embryo during swimming. Outside this range, the model was incapable of sustaining its own activity. As the excitatory drive was increased, the initial cycle period fell from about 65 ms to around 50 ms (Fig. 11*A*). Thus the level of excitatory drive had a relatively modest effect on the cycle period of the activity produced by the model.

The model was capable of generating a motor pattern for swimming when the inhibitory conductance was varied from 2 to 400 nS, a range of two orders of magnitude (Fig. 11*B*). Once again this range encompassed the plausible values for the true level of synaptic inhibition in the real circuit. The inhibitory drive proved to have a powerful influence on the cycle period of activity generated by the model. This ranged from nearly 120 ms with the inhibition at 400 nS to around 50 ms when the inhibition was set at 2 nS (Fig. 11*B*).

I also conducted an investigation as to how the cycle period varied when the strength of both the inhibition and excitation was varied simultaneously. In summary, the relationships outlined above still held true: as excitation was increased cycle period dropped no matter the level of inhibition; and as inhibition was increased the cycle period lengthened at all levels of excitation (Fig. 11*C*). This revealed that not only could the model function over a wide range of absolute values for the inhibitory and excitatory synaptic conductances but also over an even wider range when the conductances were expressed as a ratio. Thus the ratio of inhibition to excitation ranged from a minimum of 0·63 (i.e. excitation exceeding inhibition) to a maximum of 200 (Fig. 11*B* and *C*). The presumed physiological ratio for

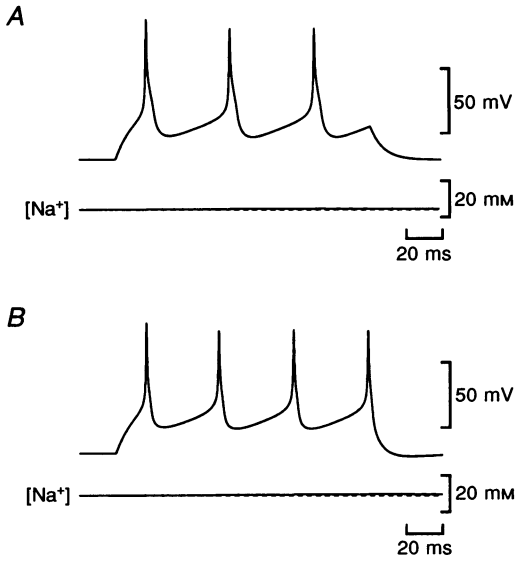

Figure 8. The Na^+-dependent K^+ current contributes to repolarization of the action potential

A, the fast K^+ current was reduced by half and submembrane $[Na^+]$ was set at 5 mM to give broader spikes. *B*, when the submembrane $[Na^+]$ was increased to 10 mM (and thus the activation of the Na^+-dependent K^+ current was increased) the spikes became narrower and membrane excitability was slightly increased.

inhibition to excitation in the real spinal circuits is probably around 10 (see above).

Can one side of the model network produce a rhythm? The real embryo can continue to generate a rhythmic motor pattern even after the two sides of the spinal cord have been surgically separated (Kahn & Roberts, 1982; Soffe, 1989) or after application of high levels of strychnine more than sufficient to completely block inhibition (Soffe, 1989). In the one-sided preparations, a combination of the voltage-dependent block of the NMDA receptor (not incorporated into the model) and the glycinergic recurrent inhibition appear to be important for rhythm generation (Soffe, 1989). I therefore tested whether the model presented here could successfully mimic both surgical division of the two sides of the spinal cord and the applications of strychnine sufficient to block all inhibition.

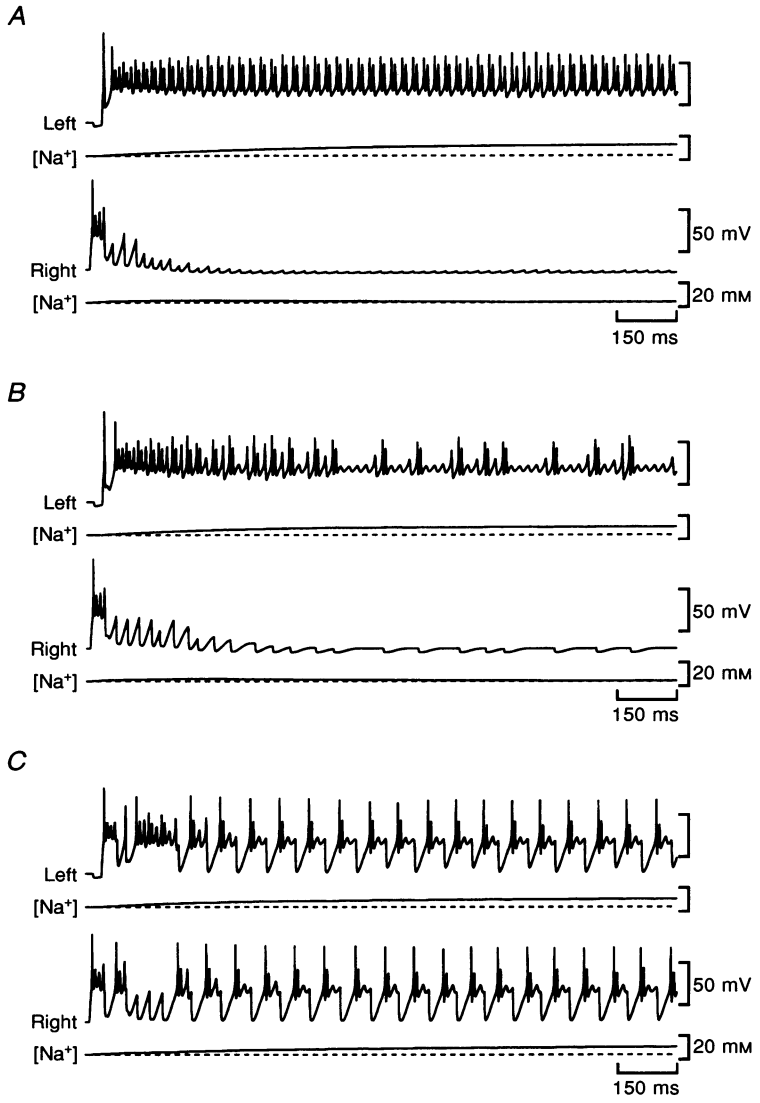

Figure 9. Complete absence of the slow K^+ current abolishes generation of the alternating pattern

Increasing the Na^+-dependent K^+ current can compensate for absence of the slow K^+ current. *A*, in the absence of the slow K^+ current and with the Na^+-dependent K^+ conductance set to 1 nS, the left neuron generated a continual burst of spikes that completely inhibited the right neuron. *B*, when the Na^+-dependent K^+ current was increased to its control value (50 nS), the left neuron still fired continually, but as submembrane Na^+ increased, some bursting in the firing pattern became evident. *C*, increasing the Na^+-dependent K^+ current to double its control value (100 nS) restored alternating firing after the submembrane Na^+ had increased sufficiently. The inhibitory conductance was 10 nS, while the non-NMDA receptor-mediated and NMDA receptor-mediated excitatory conductances were 2 nS and 1 nS, respectively.

To model surgical division, I incorporated recurrent inhibition in the model and eliminated the reciprocal inhibition. However, the model was unable to generate self-sustaining rhythmic activity unless: (1) the recurrent inhibition was set at a level that precluded alternating activity in the 'intact' model (> 3 nS); or (2) the voltage-dependent K^+ currents were reduced by at least 25%. Since surgical lesions would be unlikely to affect the level of K^+ currents, this modification is unrealistic and the model in its present state fails to give one-sided rhythm generation. However, the presence of Mg^{2+} and voltage-dependent block by NMDA receptors in the real embryo appears to be necessary for one-sided rhythm generation, and since this feature is absent from the present model it may not be surprising that it failed in this respect.

The application of high levels of strychnine (1–10 μM) was also modelled by eliminating all inhibition from the circuit. Once again, the model was unable to generate any self-sustaining activity. However, if either the fast K^+ current or both the slow and fast K^+ currents were reduced by 50%, self-sustaining rhythmic activity resulted (Fig. 12*B*). This activity had a cycle period that was roughly half that of the control network with intact inhibition (Fig. 12*A*, *B* and *C*). The cycle period was sensitive to the density of the slow K^+ current: reductions of the slow K^+ current gave shorter cycle periods (Fig. 12*C*). The change in cycle period seen in the model was remarkably similar to that seen during application of strychnine to a one-sided preparation (compare Fig. 12*C* of the present paper with Fig. 10*A* of Soffe, 1989). Thus, although K^+ currents had to be reduced, the end result appeared to be very similar to that observed with high levels of strychnine in the real embryo. Strychnine at high levels (1–10 μM) is a rather non-specific drug and blocks a variety of ion channels (Shapiro, Wang & Narahashi, 1974; Oyamo, Akaike & Carpenter, 1988) including K^+ currents in the embryo neurons (23 ± 4·5% block at 1 μM, $n = 7$, N. Dale, personal observations). Therefore, this additional reduction of the K^+ currents in the model is probably justified.

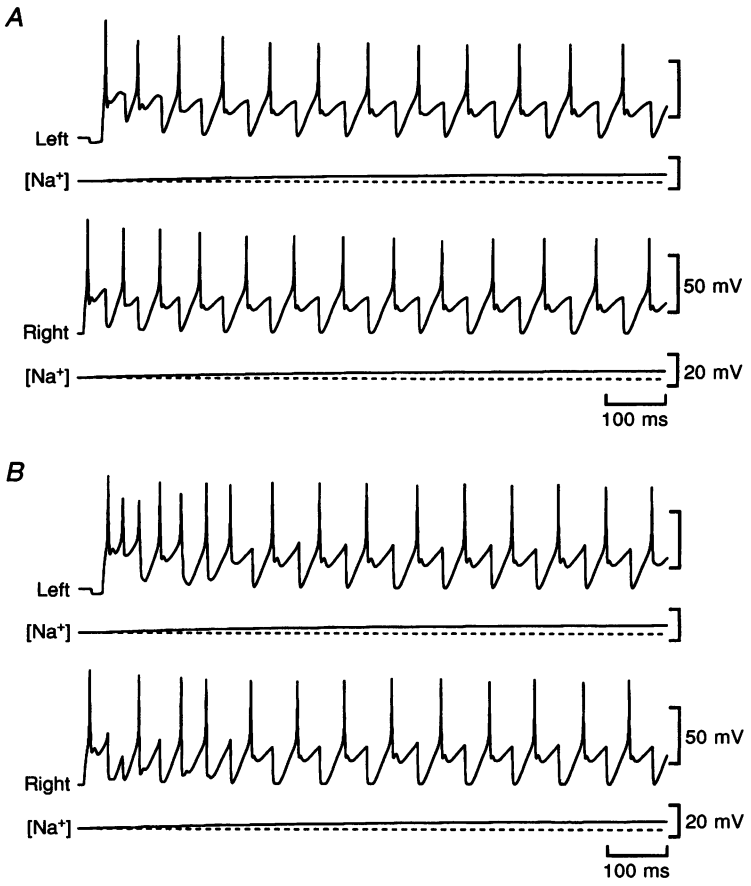

Figure 10. Introduction of recurrent inhibition into the 2-cell circuit makes the network even more sensitive to alterations of the K^+ currents

A, alternating activity in a circuit composed of control neurons, with the recurrent inhibitory conductance set at 2 nS. *B*, when the fast and slow K^+ currents were reduced by 25%, abnormalities in the motor pattern were present at the beginning of the activity. The inhibitory conductance was 10 nS, while the non-NMDA receptor-mediated and NMDA receptor-mediated excitatory conductances were 2 nS and 1 nS, respectively.

Testing the role of reciprocal inhibition in the real embryo

The model suggests that reciprocal inhibition has an important role in determining the cycle period of swimming. Since strychnine can selectively inhibit the glycinergic inhibition within the spinal network, this prediction can be readily tested by using low levels of strychnine to block the reciprocal inhibition in a graded manner.

A dose–reponse curve for strychnine was first constructed by testing its efficacy at blocking the currents evoked in isolated neurons by 100 μM glycine. Strychnine had an IC_{50} of 14 nM and thus was a very potent antagonist (Fig. 13). This was very similar to values previously reported in the literature (Cortés & Palacios, 1990). Doses of strychnine ranging from 1 to 100 nM were applied to spinal embryos and the cycle period of the swimming motor pattern was measured at the very start of the episode, 0·5 and 1 s into the episode (Fig. 14). Since all three measures gave very similar results I have presented only those measures obtained at the very start of the episode. As the levels of strychnine were increased (and thus the levels of inhibition were reduced) the cycle period became shorter (Figs 14*B* and *C* and 15*A*). This confirmed qualitatively the prediction of the model. To see whether the model could be quantitatively validated, the dose–response curve for strychnine (Fig. 13*B*) was used to convert the abscissa in Fig. 15*A*, concentration of strychnine applied, to a measure of how much inhibition remained at each dose of strychnine. This allowed cycle periods to be plotted against the amount of inhibition remaining (Fig. 15*B*).

To compare the observed relationship between reciprocal inhibition and cycle period with that predicted by the model, an absolute value for the reciprocal inhibitory conductance had to be assumed. As argued above, this is likely to be around 20–60 nS. A value of 60 nS was therefore assumed to represent the true level of inhibition, and levels of inhibition in the model smaller than 60 nS were expressed as a proportion of this level. This allowed the predictions from the model and the results from the strychnine applications to be plotted on the same graph and

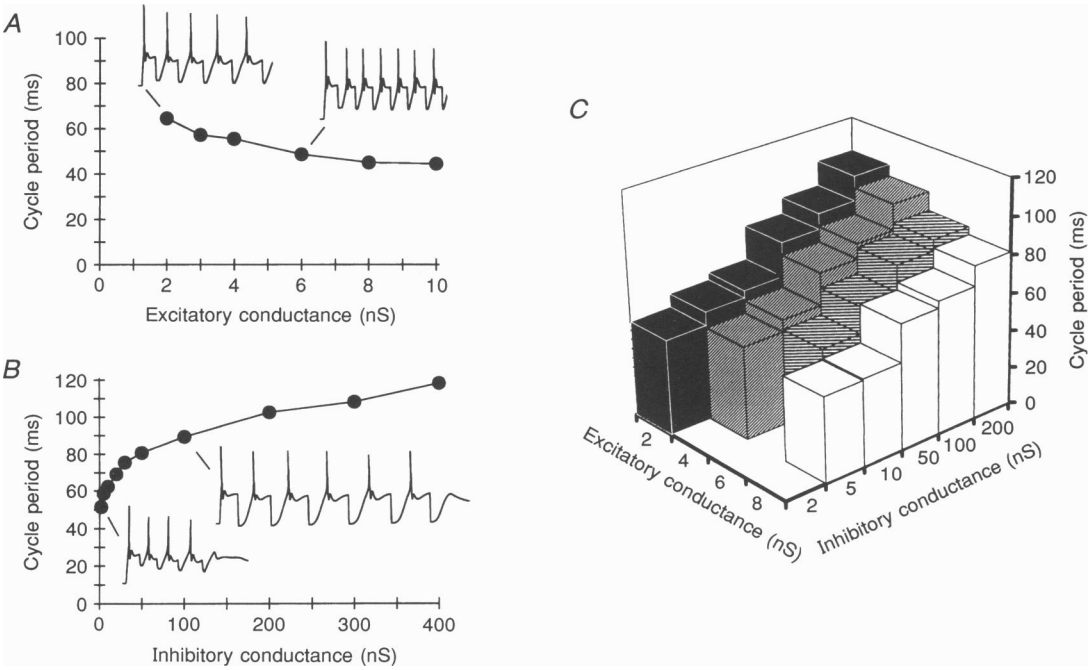

Figure 11. The 2-cell circuit can generate alternating activity over a wide range of synaptic strengths

The strength of both the excitation and inhibition determine cycle period. *A*, the excitatory conductance could be varied from 2 to 10 nS (inhibitory conductance was 10 nS) without loss of alternating activity. The cycle period grew shorter as the excitatory conductance was increased. *B*, alternating activity could be generated when the inhibitory conductance varied from 2 to 400 nS (excitatory conductance was 2 nS). The inhibitory conductance had a powerful effect on the cycle period of the activity generated by the 2-cell circuit: as inhibition was weakened, cycle period shortened. The insets in *A* and *B* show records of the activity generated by the model at selected points on the graphs. *C*, the effect of varying both the excitatory and the inhibitory conductances. Alternating activity could be generated with the ratio of the inhibitory to excitatory conductances varying from 0·63 to 200. Where a bar is missing from the graph no alternating pattern generation occurred with that combination of synaptic strengths. The magnitude of the non-NMDA component of excitation was always twice that of the NMDA component and the measures of excitatory conductance in the graphs in *A* and *C* are for the non-NMDA component only.

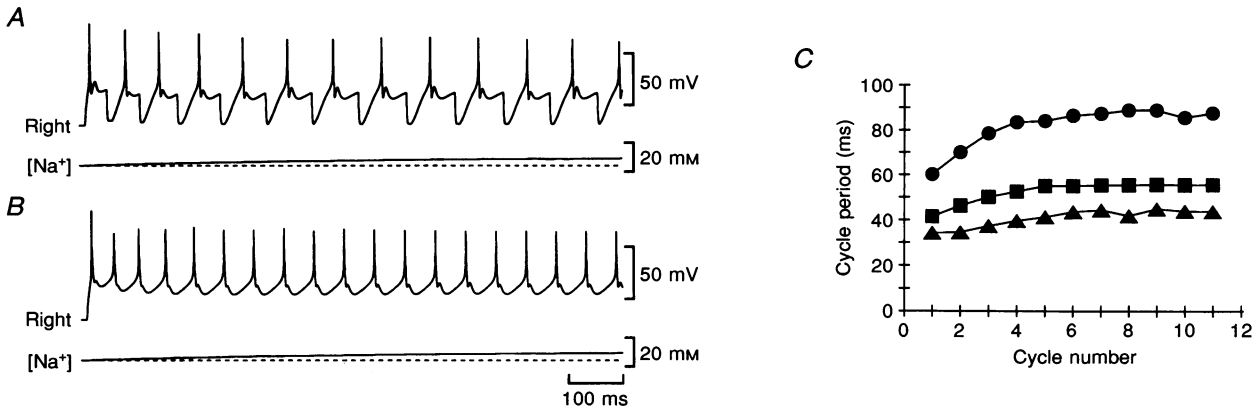

Figure 12. One side of the 2-cell circuit can produce a self-sustaining motor output

Activity of the right neuron in a 2-cell circuit in the control conditions (*A*), and after elimination of all synaptic inhibition and a reduction of the fast K^+ current by half (*B*). *C*, elimination of inhibition and halving the fast K^+ current (■) caused the cycle period of the activity to decrease by roughly half compared with the control (●). If the slow K^+ current was also halved (▲) the cycle period was decreased further. These results are very similar to the effects of large doses of strychnine that completely block inhibition and reduce K^+ currents. The inhibitory conductance was 10 nS, while the non-NMDA receptor-mediated and NMDA receptor-mediated excitatory conductances were 2 nS and 1 nS, respectively.

compared directly. When this was done, a very good correspondence was seen between the points predicted by the model and those observed during strychnine applications (Fig. 15*B*). Obviously, the true magnitude of the inhibition in the real animal will determine the degree of correspondence between model and experimental data. However, choosing control values of 20, 40 or 50 nS also gave good matches between the model predictions and the observed results.

DISCUSSION

Vertebrate locomotor systems have been modelled previously, notably the lamprey (e.g. Hellgren, Grillner & Lansner, 1992; Tråvén, Brodin, Lansner, Ekeberg, Wallén & Grillner, 1993) and the *Xenopus* embryo (Roberts & Tunstall, 1990; Wall & Dale, 1994*a*; Wolf & Roberts, 1995; Roberts *et al.* 1995). Since a systematic study of the voltage-gated channels had not been performed in either preparation, the types of channels and their kinetic parameters in these models had largely to be inferred by indirect means. This gave a large number of parameters that were essentially free and could be varied so that the model had properties similar to the system being studied. These previous models have been of considerable value in establishing that the known circuitry is sufficient (under the assumptions of the model) to generate motor patterns for swimming and have suggested possible ways in which these neural circuits may work. However, they cannot be considered as analytical tools since they contain too many free parameters. My aim has been to produce a model for a vertebrate locomotor circuit that is based much more closely on voltage-clamp data, where the ion channels present in neurons are known and specified by independently

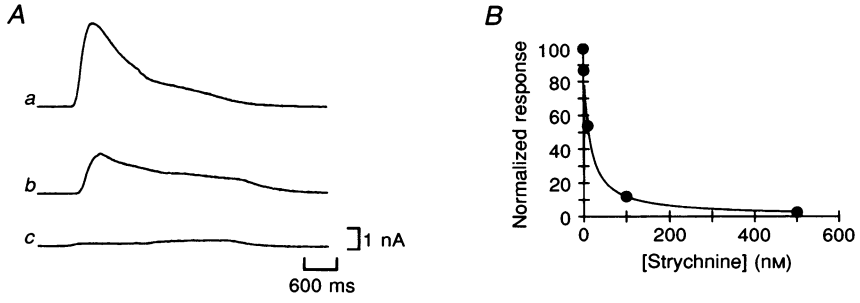

Figure 13. Dose–response relationship for strychnine *versus* glycine in acutely isolated *Xenopus* embryo spinal neurons

A, response of an isolated neuron to 100 μM glycine alone (*a*), and 100 μM glycine in the presence of 10 nM strychnine (*b*) and 100 nM strychnine (*c*). *B*, dose–response curve consisting of pooled data from 5 neurons. The IC_{50} for strychnine was 14 nM.

measured kinetic parameters. This has the effect of greatly limiting the free parameters in the model available for manipulation by the investigator. Indeed, in the model presented in this paper, only the neuronal input resistance and magnitudes of the ionic and synaptic conductances can be varied as free parameters. Even these parameters are limited either to experimentally observed ranges (in the case of the input resistance and magnitude of the voltage-gated currents) or to physiologically plausible ranges (the synaptic conductances). A model that is restricted in this way is capable, first, of determining whether the mechanisms studied in the real animal and incorporated into the model can adequately explain generation of the motor pattern. Second, the model can be used to make predictions that are testable experimentally and thus validate the model. Finally, a fully validated model can be

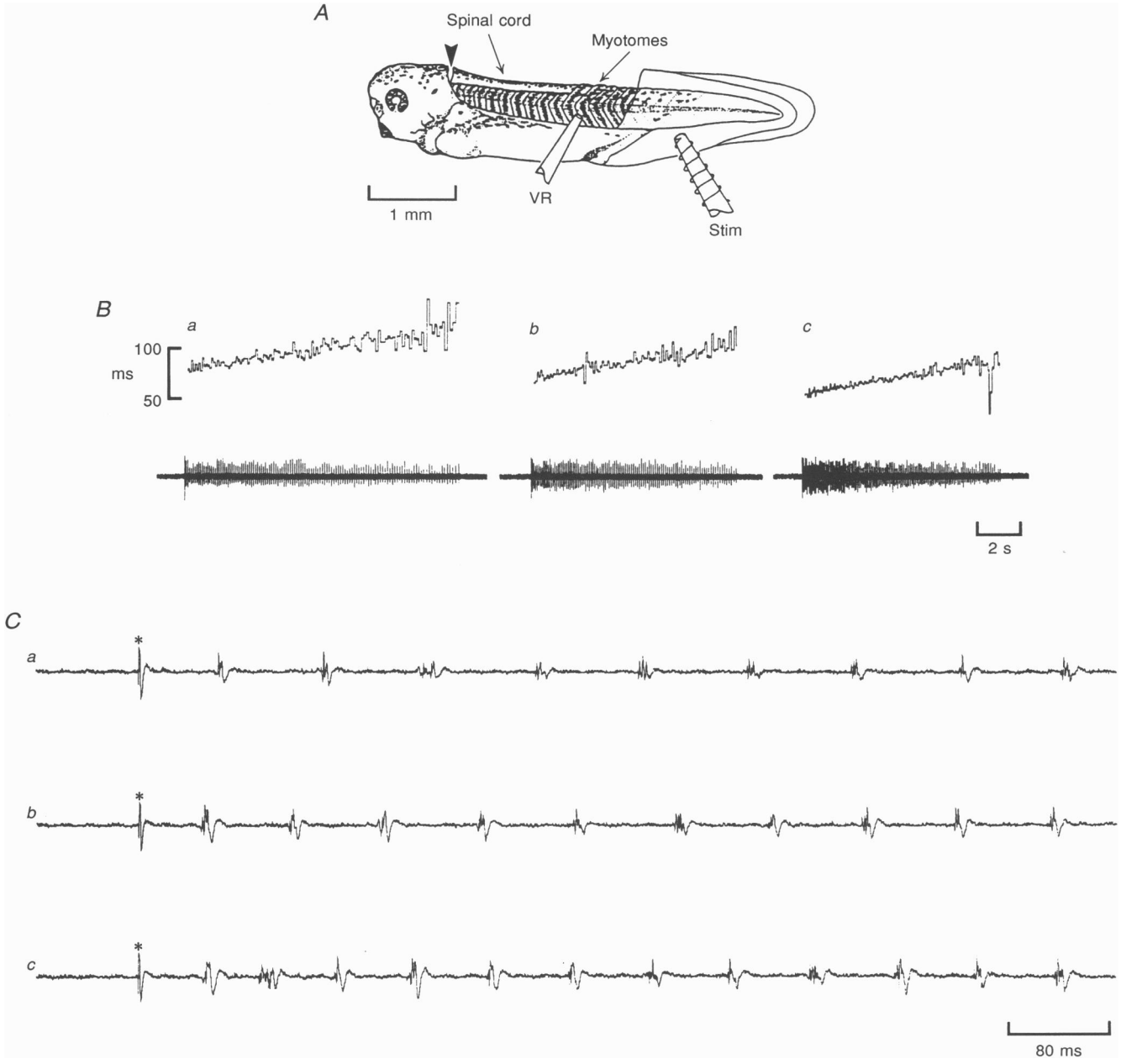

Figure 14. Application of strychnine to the embryo shortens the cycle period of swimming

A, diagram of the preparation to show position of stimulating (Stim) and ventral root recording (VR) electrodes. The spinal cord was transected at the arrowhead. *B*, sample records from 1 embryo showing ventral root activity (VR) and cycle period (upper trace) during the control period (*a*), and in the presence of 10 nM strychnine (*b*) and 100 nM strychnine (*c*). Note how strychnine shortens cycle periods throughout the swimming episode. *C*, expanded portions of the beginning of the records in *B* showing the initial cycle period in the control conditions (*a*), and in the presence of 10 nM strychnine (*b*) and 100 nM strychnine (*c*). The asterisks indicate electrical artefacts caused by stimulation of skin.

used with much greater confidence as a tool to analyse how a neural circuit works. It is important to remember that, although limited by the observed physiological range, the choice of values for the input resistance and magnitude of ionic conductances is arbitrary. Different values from within the physiological range would have given somewhat different results with respect to details, but would not alter the main conclusions and predictions of this paper.

Previous modelling studies of the *Xenopus* embryo

Previous simulations of the *Xenopus* embryo spinal circuitry have used neurons that possessed just two channels: a Na^+ and K^+ channel. The kinetic parameters for these channels were based upon those of the squid giant axon and modified to give the modelled neurons similar firing and membrane properties to those observed during intracellular recording from *Xenopus* neurons (Roberts & Tunstall, 1990; Wolf & Roberts, 1995; Roberts *et al.* 1995). Remarkably, these highly simplified models were able to produce an alternating motor pattern somewhat similar to that seen in the real embryo. The cycle periods of the alternating activity produced by these models varied from around 40 to 70 ms. In earlier versions of these models, increasing the excitatory synaptic conductance gave a modest shortening of cycle period, whereas the cycle period was rather insensitive to the strength of the inhibitory synaptic conductance (Roberts & Tunstall, 1990). More recent simulation studies have suggested that both the inhibitory and excitatory conductances could exert modest control over cycle period (Wolf & Roberts, 1995; Roberts *et al.* 1995).

However, these previous models are unable to replicate many of the known features of the system. In the model neurons the spikes during rhythmic activity are about half the amplitude of the initial spike (Roberts & Tunstall, 1990; Wolf & Roberts, 1995; Roberts *et al.* 1995). This is not an observed feature of the activity of spinal neurons during fictive swimming. These models cannot: (1) reproduce the whole range of cycle periods seen in the real embryo (Roberts & Tunstall, 1990; Wolf & Roberts, 1995; Roberts *et al.* 1995); (2) mimic the actions of K^+ channel blockers on motor pattern generation unless the magnitudes of the voltage-gated currents are increased 5-fold (Wall & Dale, 1994*a*); and (3) explain how the spinal circuitry can generate a rhythmic output in the absence of inhibition (Roberts & Tunstall, 1990).

In the new model presented here, both the complement of channels and their kinetic parameters are based upon voltage-clamp data from isolated *Xenopus* neurons (Dale, 1995) and are very different from those used in previous simulations of the *Xenopus* embryo spinal network (Roberts & Tunstall, 1990; Wall & Dale, 1994*a*; Roberts *et al.* 1995; Wolf & Roberts, 1995). Ideally, these experimentally determined values for the kinetic parameters and the types of channels present should be used in all future simulations of this system.

The new model can replicate many features of the swimming motor pattern

The highly simplified model network presented here, consisting of only two neurons, was able to replicate many aspects of the motor pattern for swimming observed in real embryos.

First, the model could generate the basic alternating pattern characteristic of swimming, with cycle periods that encompassed the whole range observed in real embryos.

Second, reductions of voltage-gated K^+ currents could mimic the known actions of non-selective K^+ channel blockers and produce very similar perturbations in the

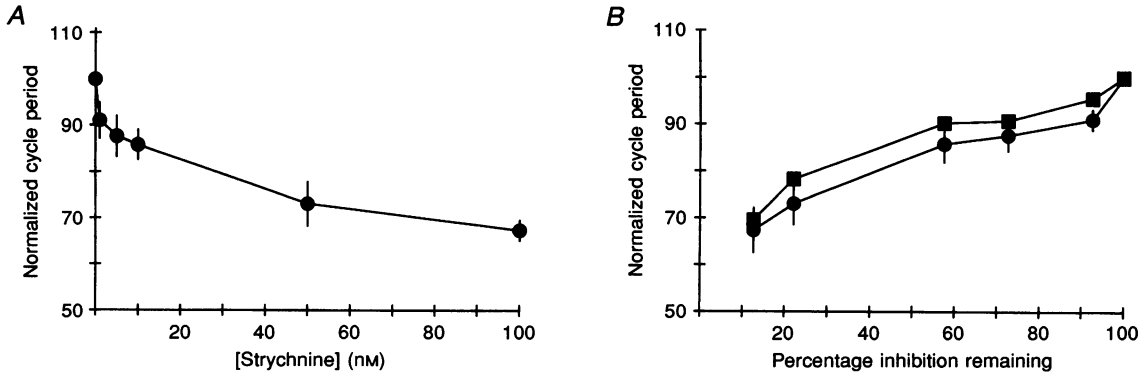

Figure 15. Cycle period depends upon the strength of the glycinergic inhibition in a manner predicted by the model

A, pooled data from 5 embryos showing how cycle period varies as the concentration of strychnine is increased. *B*, the data in *A* replotted by using the strychnine dose–response curve to recalculate the abscissa as percentage inhibition remaining to show directly the relationship between the inhibitory conductance and cycle period in the real animal (●). The bars represent 1 S.E.M. The values for cycle period predicted from the model (■) plotted against percentage inhibition remaining, assuming that the control inhibitory conductance was 60 nS, closely correspond to the experimental values.

motor pattern. The reductions needed to produce these perturbations in the model were somewhat larger than those seen with the K^+ channel blockers in the real embryo. However, introduction of a modest amount of recurrent inhibition into the circuit (present to some degree in the real embryo, Dale, 1985) made the model much more sensitive to reduction of K^+ currents. Furthermore, reductions of the K^+ currents in the model gave abnormal cycles only at the beginning of the motor activity and spontaneous transitions between the various abnormal patterns and the normal pattern. This was very similar to the effects of K^+ channel blockers in the real embryo (Wall & Dale, 1994*a*). Previous simulations could accurately reproduce the actions of K^+ channel blockers only by using bigger networks of four or eight cells and altering the amplitudes of K^+ currents in subsets of the neurons (Wall & Dale, 1994*a*).

Third, the model could generate rhythmic activity in the absence of inhibition if the K^+ currents were also reduced. This manipulation mimics the action of strychnine, since at high doses it not only abolishes the inhibition (see also Dale, 1985) but blocks K^+ currents. The cycle period of this rhythmic activity was very similar to that seen during complete blockade of inhibition by strychnine.

Fourth, the strength of reciprocal inhibition in the model proved to be a powerful determinant of the cycle period of the activity. This prediction was quantitatively validated by the use of strychnine to block the reciprocal inhibition in the real embryo in a graded manner.

In addition, the modelled neurons had membrane properties that were similar to those of the real neurons: they exhibited strong membrane rectification over the correct voltage range and their repetitive firing properties were controlled by both the Ca^{2+} current and the K^+ currents (as described in real neurons, Soffe, 1990; Dale, 1991; Wall & Dale, 1994*b*). Furthermore, although the modelled neurons fired repetitively much more readily than neurons recorded with sharp microelectrodes, this discrepancy could be reconciled if the shunting of the membrane introduced by the microelectrode was incorporated into the model.

Predictions from the model

The model makes several predictions.

First, the fast K^+ current determines spike width while the slow K^+ current determines the repetitive firing properties of the spinal neurons.

Second, damage by the microelectrode significantly reduces the membrane excitability of the spinal neurons and changes their activity pattern during fictive locomotion.

Third, the slow K^+ current is essential for motor pattern generation and a selective and complete blockade of this current should abolish the motor pattern.

Fourth, intracellular Na^+ builds up rapidly over the first 1 s of motor activity. The Na^+-dependent K^+ current could contribute to both spike repolarization and activity-dependent negative feedback within the locomotor circuit.

Fifth, the strength of the excitation and particularly the reciprocal inhibition are important determinants of the cycle period of rhythmic activity.

Sixth, motor patterns that entail high frequency repetitive firing either in *Xenopus* (e.g. struggling, Soffe, 1993; or the larval motor pattern, Sillar, Simmers & Wedderburn, 1992) or those closely related amphibian embryos such as *Rana* or *Triturus* (Soffe, Clarke & Roberts, 1983; Soffe & Sillar, 1991) may involve a weakening of the slow K^+ current to allow such high frequency repetitive firing to occur.

All of these predictions are amenable to experimental testing; indeed, the relationship between the reciprocal inhibition and cycle period has already been tested. The use of a less invasive recording technique, such as whole-cell patch clamp, from neurons in the spinal cord will be an important test of whether the shunting action of the microelectrode changes neuronal membrane properties and the details of the motor pattern for swimming in spinal neurons. Clearly, identification of a specific pharmacological blocker for the slow K^+ current is very important to allow the role of this key current to be tested experimentally in the real embryo.

Features missing from the model and scope for its improvement

Several features of the real system are missing from the model. First, not all of the known ionic currents present in *Xenopus* neurons have been incorporated into the model. At least some of the *Xenopus* spinal neurons possess an A-type K^+ current (Ribera & Spitzer, 1990; N. Dale personal observations) as well as a transient Ca^{2+} current (Gu & Spitzer, 1993). While these currents are likely to be minor components, the vast majority of spinal neurons possess a slowly activating Ca^{2+}-dependent K^+ current (Wall & Dale, 1995). The absence of this current is a much more serious omission from the model. The slow time-dependent inactivation of the K^+ and Ca^{2+} currents has also been omitted. While the absence of the Ca^{2+}-dependent K^+ current and the slow inactivation of the K^+ and Ca^{2+} currents probably does not matter for simulation of short segments of motor activity, their absence means that the model cannot successfully reproduce the time-dependent changes in cycle period and the spontaneous termination of activity seen in the real embryo (Kahn & Roberts, 1982; Wall & Dale, 1995). Analysis of these slow changes in the motor pattern awaits introduction of these mechanisms.

Second, no voltage-dependent blockade of the NMDA receptor by Mg^{2+} was incorporated. This is probably not a serious omission: the embryo can swim perfectly well in the absence of Mg^{2+}, and its re-introduction has only minor effects in the real embryo (Soffe & Roberts, 1989). However,

the presence of Mg^{2+} seems much more important after surgical division of the two halves of the spinal cord (Soffe, 1989) and the successful modelling of this manipulation may require incorporation of blockade of the NMDA receptor by Mg^{2+}.

Third, the neurons were modelled by a single compartment. This is certainly a reasonable approximation since *Xenopus* embryo spinal neurons possess only relatively few very short dendrites (Roberts & Clarke, 1982; Soffe, Clarke & Roberts, 1984; Dale, 1985; Roberts *et al.* 1988). However, some electrophysiological evidence exists that can be interpreted as showing the existence of at least two compartments: the decay of the membrane potential in response to hyperpolarizing current injection contains two exponential components (Soffe, 1989). Previous simulations of the *Xenopus* spinal network have incorporated as many as three compartments into each neuron (Roberts & Tunstall, 1990; Roberts *et al.* 1995; Wolf & Roberts, 1995). However, the single-compartment model presented here is much more successful at simulating the motor pattern for swimming than these previous models and the increase in realism gained by incorporating extra compartments into the model may not be worth the considerable extra computational overhead that this feature would entail.

Fourth, the networks I have simulated so far have only consisted of two or three neurons. Considerable extra realism would result from simulating larger numbers of neurons, especially if the artificial dual-function neurons of this simulation were split into separate excitatory and inhibitory interneurons (cf. Fig. 4). Indeed, real neurons vary in their density of ionic currents (Table 1) and input resistances and capacitances. Simulations involving larger numbers of neurons would enable a study of how networks composed of non-identical neurons function. In the lamprey, introduction of heterogeneity of this sort stabilizes circuit operation (Hellgren, Grillner & Lansner, 1992). Such simulations of the *Xenopus* locomotor circuits may reproduce the effects of K^+ channel blockers better, allow more successful simulation of the workings of one side of the spinal cord and permit investigation of how populations of neurons can be recruited and derecruited from the circuit (cf. Sillar & Roberts, 1993; Wolf & Roberts, 1995). In addition, the simplifying assumption was made that all the neurons have essentially the same properties. While no evidence exists to the contrary, future experimental work may reveal differences between the properties of classes of neurons that would have to be incorporated into the simulations.

Finally, the networks simulated in this paper had a simplified system of synaptic connectivity. In the real embryos, motoneurons make central nicotinic synapses onto other motoneurons and interneurons as well as electrical junctions with other motoneurons (Perrins & Roberts, 1995*a*, *b*). These connections were omitted from the model. This is probably justifiable, since the real embryo can generate the motor pattern for swimming even when the central nicotinic synapses are blocked by antagonists (Perrins & Roberts, 1995*b*). The contribution of the electrical connections between motoneurons remains uncertain but is likely to boost the phasic excitation in motoneurons during fictive locomotion. Clearly, incorporation of electrical coupling into the model would help in the investigation of its possible roles.

How does the central pattern generator for swimming work?

Previous models of the locomotor network in the *Xenopus* embryo (not based upon voltage clamp data) have been composed of neurons capable of firing only single spikes in response to current injection (Roberts & Tunstall, 1990; Roberts *et al.* 1995; Wolf & Roberts, 1995). This has given rise to the idea that this property of strong membrane accommodation is important for the correct operation of the circuit (Roberts & Tunstall, 1990). Furthermore, it has been proposed that postinhibitory rebound also plays a key role in motor pattern generation (Roberts & Tunstall, 1990; Roberts *et al.* 1995). The new model based upon experimental data and presented in this paper suggests that these ideas may have to be revised.

The property of strong membrane accommodation may be an artefact that results from damage to the neuron during intracellular recordings. Indeed, despite the ability of the model neurons to fire repetitively, the model network could still generate the motor pattern for swimming. Together, these observations suggest that membrane accommodation is not an important feature for operation of the circuit. The model could generate the motor pattern for swimming over a range of ratios of the inhibitory to excitatory conductances that varied by more than 300-fold. This suggests that while the reciprocal inhibition helps to remove the inactivation of the Na^+ channels (and thus contribute to postinhibitory rebound), it need only be present in very small quantities. In the real embryo, motor pattern generation can take place with only very weak inhibition present in the circuit (Soffe & Roberts, 1982; Soffe, 1989; Figs 14 and 15*B*). Both these factors suggest that while postinhibitory rebound may play a role in the function of the circuit there may be a much lesser requirement for it than proposed in previous models (Roberts & Tunstall, 1990; Roberts *et al.* 1995; Wolf & Roberts, 1995).

What are the key features of the new model that may explain why the circuit generates a motor pattern typical of the embryo? During current injection, the model neurons fire with interspike intervals ranging from 35 to 50 ms (Figs 1*A* and 2). This interval is roughly half the typical cycle period for swimming and depends largely upon the magnitude and properties of the slow K^+ current. This tendency to fire at frequencies roughly double those typical of swimming motor activity is thus an intrinsic feature of the model neurons. It becomes rather easy to understand how two populations of neurons possessing this feature can

be coupled together by reciprocal inhibition to give alternating activity at a frequency that is about half that of the intrinsic firing frequency: each side is being inhibited around the time that they would naturally tend to fire a further spike. On this hypothesis, the slow K^+ current, which is largely responsible for setting this intrinsic rate of firing, is vital for the production of the swimming motor pattern and could be considered as the 'pacemaker current' for swimming. In the complete absence of the slow K^+ current, motor pattern generation in the model fails unless other K^+ currents are increased to possibly unphysiological levels (Fig. 9). This hypothesis would also explain why one side of the spinal cord can generate rhythmic activity at roughly double the frequency of swimming: the neurons in the absence of reciprocal inhibition are reverting to their intrinsic firing pattern.

In the model, the network could generate alternating motor patterns over a very wide range of synaptic strengths. At one extreme the excitation could be almost double the reciprocal inhibition, while at the other the inhibition could be 200 times bigger than the excitation. The synaptic connectivity could therefore be considered merely as a device for sustaining activity within the circuit, getting the spinal neurons to fire at rates close to their intrinsic frequencies and coupling the antagonistic motor centres to co-ordinate the alternating activity. The magnitudes of the synaptic drive may thus be of relatively little importance in rhythm generation itself other than to determine the cycle period of the motor activity. By contrast, motor pattern generation in the model, and indeed the real embryo (Wall & Dale, 1994*a*), is much more sensitive to the balance between the inward and outward currents: reductions of the K^+ currents by as little as 20% can disrupt the motor pattern.

This result has interesting implications for development of the central pattern generator for swimming. Neurons within the spinal network receive inputs from several convergent inhibitory and excitatory interneurons as well as motoneurons (Dale & Roberts, 1985; Wall & Dale, 1993; Sillar & Roberts, 1993; Perrins & Roberts, 1995*b*). The number of presynaptic interneurons converging on a single neuron within the circuit will obviously be an important determinant of the strength of the total inhibitory and excitatory synaptic drive received by that neuron. Since the model is rather insensitive to the levels of synaptic drive, the real circuit may be able to tolerate considerable variation in the number of convergent synaptic inputs per neuron while still preserving the capacity for motor pattern generation. However, both the model and the real circuit are very sensitive to alterations of the balance between the voltage-gated currents. For correct motor pattern generation to occur, there may have to be mechanisms that regulate the relative levels of expression of several different channels rather precisely (cf. Lindsell & Moody, 1994). The challenge in understanding how neural circuits develop correctly may thus lie not in understanding the details of how synaptic connections are developmentally regulated but rather in how the correct balance in the expression of an array of ionic channels is achieved.

Implications for the generation of other motor patterns

The *Xenopus* embryo can generate an alternative motor pattern, struggling, that is characterized by bursts of repetitive firing in spinal neurons (Kahn & Roberts, 1982; Soffe, 1993). During later development, the motor pattern for swimming in the larva starts to involve neurons firing bursts of spikes (Sillar *et al.* 1992). Related amphibian embryos, such as those of *Rana* or *Triturus*, also have motor patterns that involve neurons firing spikes in bursts rather than singly, as is typical of swimming in the *Xenopus* embryo (Soffe *et al.* 1983; Soffe & Sillar, 1991). Given that the slow K^+ current exerts a powerful influence over the frequency of firing, how can these related motor patterns be generated? The results presented here suggest that the magnitude of the slow current must be regulated. In the case of struggling the slow current may be reduced by neuromodulation. For the *Xenopus* larva or the *Rana* embryo there may be developmental regulation so that the slow K^+ current is smaller relative to the other currents of the neurons. In the preceding paper (Dale, 1995), I tentatively identified the slow K^+ current as the slow current that develops first in the 'young' embryonic neurons (O'Dowd, Ribera & Spitzer, 1988). At early stages of development this current is thought to constitute a larger proportion of the total outward current and as development proceeds it may constitute a smaller and smaller proportion (O'Dowd *et al.* 1988). Should this process continue into the larval stages of development it may permit a higher frequency of firing and thus generation of the larval motor pattern. Similarly, it may be that *Rana* neurons express relatively less of this slow K^+ current.

Arshavsky, Y. I., Orlovsky, G. N., Panchin, Y. V., Roberts, A. & Soffe, S. R. (1993). Neuronal control of swimming locomotion: analysis of the pteropod mollusc *Clione* and embryos of the amphibian *Xenopus*. *Trends in Neurosciences* **16**, 227–233.

Clarke, J. D. W. & Roberts, A. (1984). Interneurones in the *Xenopus* embryo spinal cord: sensory excitation and activity during swimming. *Journal of Physiology* **354**, 345–362.

Cortés, R. & Palacios, J. M. (1990). Autoradiographic mapping of glycine receptors by [^{3}H] strychnine binding. In *Glycine Neurotransmission*, ed. Ottersen, O. P. & Storm-Mathisen, J., pp. 239–263. Wiley, Chichester, UK.

Dale, N. (1985). Reciprocal inhibitory interneurons in the *Xenopus* embryo spinal cord. *Journal of Physiology* **363**, 61–70.

Dale, N. (1991). The isolation and identification of spinal neurons that control movement in the *Xenopus* embryo. *European Journal of Neuroscience* **3**, 1025–1035.

Dale, N. (1993). A large, sustained Na^+- and voltage-dependent K^+ current in spinal neurons of the frog embryo. *Journal of Physiology* **462**, 349–372.

DALE, N. (1995). Kinetic characterization of the voltage-gated currents possessed by *Xenopus* embryo spinal neurons. *Journal of Physiology* **489**, 473–488.

DALE, N. & ROBERTS, A. (1984). Excitatory amino acid receptors in *Xenopus* embryo spinal cord and their role in activation of swimming. *Journal of Physiology* **348**, 527–543.

DALE, N. & ROBERTS, A. (1985). Dual-component amino-acid-mediated synaptic potentials: Excitatory drive for swimming in *Xenopus* embryos. *Journal of Physiology* **363**, 35–59.

DICKINSON, P. (1989). Modulation of simple motor patterns. *Seminars in the Neurosciences* **1**, 15–24.

FORSYTHE, I. D. & WESTBROOK, G. L. (1988). Slow excitatory postsynaptic currents mediated by *N*-methyl-D-aspartate receptors on cultured mouse central neurons. *Journal of Physiology* **396**, 515–533.

GETTING, P. A. (1989). Reconstruction of small neural networks. In *Methods in Neuronal Modelling, from Synapses to Networks*, ed. KOCH, C. & SEGEV, I., pp. 171–194. MIT Press, Cambridge, MA, USA and London, UK.

GU, X. & SPITZER, N. C. (1993). Low-threshold Ca^{2+} current and its role in spontaneous elevations of intracellular Ca^{2+} in developing *Xenopus* neurons. *Journal of Neuroscience* **13**, 4936–4948.

HELLGREN, J., GRILLNER, S. & LANSNER, A. (1992). Computer simulation of the segmental neural network generating locomotion in the lamprey using populations of network interneurons. *Biological Cybernetics* **68**, 1–13.

HILL, R., MATSUSHIMA, T., SCHOTLAND, J. & GRILLNER, S. (1992). Apamin blocks the slow AHP in lamprey and delays termination of locomotor bursts. *NeuroReport* **3**, 943–945.

KAHN, J. A. & ROBERTS, A. (1982). The central nervous origin of the swimming motor pattern in embryos of *Xenopus laevis*. *Journal of Experimental Biology* **99**, 185–196.

KORN, H. & FABER, D. S. (1990). Quantitative electrophysiological studies and modelling of central glycinergic synapses. In *Glycine Neurotransmission*, ed. OTTERSEN, O. P. & STORM-MATHISEN, J., pp. 139–170. Wiley, Chichester, UK.

KORN, H., TRILLER, A., MALLET, A. & FABER, D. S. (1981). Fluctuating responses at a central synapse: n of binomial fit predicts the number of stained presynaptic boutons. *Science* **213**, 898–901.

LINDSELL, P. & MOODY, W. J. (1994). Na^+ channel mis-expression accelerates K^+ channel development in embryonic *Xenopus laevis* muscle. *Journal of Physiology* **480**, 405–410.

MCCORMICK, D. A. & HUGUENARD, J. R. (1992). A model of the electrophysiological properties of thalamocortical relay neurons. *Journal of Neurophysiology* **68**, 1384–1400.

NIEUWKOOP, P. D. & FABER, J. (1956). *Normal Tables of Xenopus laevis (Daudin)*. North Holland, Amsterdam.

O'DOWD, D. K., RIBERA, A. B. & SPITZER, N. C. (1988). Development of voltage-dependent calcium, sodium and potassium currents in *Xenopus* spinal neurons. *Journal of Neuroscience* **8**, 792–805.

OYAMA, Y., AKAIKE, N. & CARPENTER, D. O. (1988). Strychnine decreases the voltage-dependent Ca^{2+} current of both *Aplysia* and frog ganglion neurons. *Cellular and Molecular Neurobiology* **8**, 307–314.

PERRINS, R. J. & ROBERTS, A. (1995*a*). Cholinergic and electrical synapses between synergistic motoneurones in the *Xenopus laevis* embryo. *Journal of Physiology* **485**, 135–144.

PERRINS, R. J. & ROBERTS, A. (1995*b*). Cholinergic contribution to excitation in a spinal locomotor central pattern generator in *Xenopus* embryos. *Journal of Neurophysiology* **73**, 1013–1019.

PRESS, W. H., FLANNERY, B. P., TEUKOLSKY, S. A. & VETTERLING, W. T. (1988). *Numerical Recipes in C. The Art of Scientific Computing*. Cambridge University Press, Cambridge, UK.

REDMAN, S. & WALMSLEY, B. (1983). Amplitude fluctuations in synaptic potentials evoked in cat spinal motoneurons at identified group I a synapses. *Journal of Physiology* **343**, 135–145.

RIBERA, A. B. & SPITZER, N. C. (1990). Differentiation of I_{K_A} in amphibian spinal neurons. *Journal of Neuroscience* **10**, 1886–1891.

ROBERTS, A. & CLARKE, J. D. W. (1982). The neuroanatomy of an amphibian embryo spinal cord. *Philosophical Transactions of the Royal Society* B **296**, 195–212.

ROBERTS, A., DALE, N., OTTERSEN, O. P. & STORM-MATHISEN, J. (1988). Development and characterization of commissural interneurons in the spinal cord of *Xenopus laevis* embryos revealed by antibodies to glycine. *Development* **103**, 447–461.

ROBERTS, A. & KAHN, J. A. (1982). Intracellular recordings from spinal neurons during "swimming" in paralysed amphibian embryos. *Philosophical Transactions of the Royal Society* B **296**, 213–228.

ROBERTS, A. & SILLAR, K. T. (1990). Characterization and function of spinal excitatory interneurons with commissural projections in *Xenopus laevis* embryos. *European Journal of Neuroscience* **2**, 1051–1062.

ROBERTS, A. & TUNSTALL, M. J. (1990). Mutual re-excitation with post inhibitory rebound: a simulation study on the mechanisms for locomotor generation in the spinal cord of *Xenopus* embryos. *European Journal of Neuroscience* **2**, 11–23.

ROBERTS, A., TUNSTALL, M. J. & WOLF, E. (1995). Properties of networks controlling locomotion in a simple vertebrate and significance of voltage-dependency of NMDA channels: a simulation study of rhythm generation sustained by positive-feedback. *Journal of Neurophysiology* **73**, 485–495.

SELVERSTON, A. I. (1980). Are central pattern generators understandable? *Behavioural and Brain Sciences* **3**, 535–571.

SHAPIRO, B. I., WANG, C. M. & NARAHASHI, T. (1974). Effects of strychnine on ionic conductances of squid giant axon membrane. *Journal of Pharmacology and Experimental Therapeutics* **188**, 66–76.

SILLAR, K. T. & ROBERTS, A. (1992). The role of premotor interneurons in phase-dependent modulation of a cutaneous reflex during swimming in *Xenopus laevis* embryos. *Journal of Neuroscience* **12**, 1647–1657.

SILLAR, K. T. & ROBERTS, A. (1993). Control of frequency during swimming in *Xenopus* embryos: a study on interneuronal recruitment in a spinal rhythm generator. *Journal of Physiology* **472**, 557–572.

SILLAR, K. T., SIMMERS, A. J. & WEDDERBURN, J. F. S. (1992). The post-embryonic development of cell properties and synaptic drive underlying locomotor rhythm generation in *Xenopus* larvae. *Proceedings of the Royal Society* B **249**, 65–70.

SOFFE, S. R. (1987). Ionic and pharmacological properties of reciprocal inhibition in *Xenopus* embryo motoneurons. *Journal of Physiology* **382**, 463–473.

SOFFE, S. R. (1989). Roles of glycinergic inhibition and *N*-methyl-D-aspartate receptor mediated excitation in the locomotor rhythmicity of one half of the *Xenopus* embryo central nervous system. *European Journal of Neuroscience* **1**, 561–571.

SOFFE, S. R. (1990). Active and passive membrane properties of spinal cord neurones that are rhythmically active during swimming in *Xenopus* embryos. *European Journal of Neuroscience* **2**, 1–10.

SOFFE, S. R. (1991). The triggering and gating of motor responses by sensory stimulation: behavioural selection in *Xenopus* embryos. *Proceedings of the Royal Society* B **246**, 197–203.

SOFFE, S. R. (1993). Two distinct rhythmic motor patterns are driven by common premotor and motor neurons in a simple vertebrate spinal cord. *Journal of Neuroscience* **13**, 4456–4469.

SOFFE, S. R., CLARKE, J. D. W. & ROBERTS, A. (1983). Swimming and other centrally generated motor patterns in newt embryos. *Journal of Comparative Physiology* A **152**, 535–544.

SOFFE, S. R., CLARKE, J. D. W. & ROBERTS, A. (1984). Activity of commissural interneurons in spinal cord of *Xenopus* embryos. *Journal of Neurophysiology* **51**, 1257–1267.

SOFFE, S. R. & ROBERTS, A. (1982). Tonic and phasic synaptic input to spinal cord motoneurons during fictive locomotion in frog embryos. *Journal of Neurophysiology* **48**, 1279–1288.

SOFFE, S. R. & ROBERTS, A. (1989). The influence of magnesium ions on the NMDA mediated responses of ventral rhythmic neurons in the spinal cord of *Xenopus* embryos. *European Journal of Neuroscience* **1**, 507–515.

SOFFE, S. R. & SILLAR, K. T. (1991). Patterns of synaptic drive to ventrally located spinal neurons in *Rana temporaria* embryos during rhythmic and non-rhythmic motor responses. *Journal of Experimental Biology* **156**, 101–118.

TIERNEY, A. J. & HARRIS-WARRICK, R. M. (1992). Physiological role of the transient potassium current in the pyloric circuit of the lobster stomatogastric ganglion. *Journal of Neurophysiology* **67**, 599–609.

TRAUB, R. D., WONG, R. K. S., MILES, R. & MICHELSON, H. (1991). A model of a CA3 hippocampal pyramidal neuron incorporating voltage-clamp data on intrinsic conductances. *Journal of Neurophysiology* **66**, 635–650.

TRÅVÉN, H. G. C., BRODIN, L., LANSNER, A., EKEBERG, Ö., WALLÉN, P. & GRILLNER, S. (1993). Computer simulations of NMDA and non-NMDA receptor-mediated synaptic drive: sensory and supraspinal modulation of neurons and small networks. *Journal of Neurophysiology* **70**, 695–709.

TUNSTALL, M. J. & ROBERTS, A. (1994). A longitudinal gradient of synaptic drive in the spinal cord of *Xenopus* embryos and its role in the co-ordination of swimming. *Journal of Physiology* **474**, 393–405.

WALL, M. J. & DALE, N. (1993). $GABA_B$ receptors modulate glycinergic inhibition and spike threshold in *Xenopus* embryo spinal neurons. *Journal of Physiology* **469**, 275–290.

WALL, M. J. & DALE, N. (1994*a*). A role for potassium currents in the generation of the swimming motor pattern of *Xenopus* embryos. *Journal of Neurophysiology* **72**, 337–348.

WALL, M. J. & DALE, N. (1994*b*). $GABA_B$ receptors modulate an ω-conotoxin sensitive calcium current which is required for synaptic transmission in the *Xenopus* embryo spinal cord. *Journal of Neuroscience* **14**, 6248–6255.

WALL, M. J. & DALE, N. (1995). A slowly activating Ca^{2+}-dependent K^+ current that plays a role in termination of swimming in *Xenopus* embryos. *Journal of Physiology* **487**, 557–572.

WOLF, E. & ROBERTS, A. (1995). The influence of premotor interneuron populations on the frequency of the spinal pattern generator for swimming in *Xenopus* embryos: a simulation study. *European Journal of Neuroscience* **7**, 671–678.

Acknowledgements

I thank Dr S. R. Soffe for reading an earlier version of this paper and the Royal Society and SERC for generous support.

Received 6 December 1994; accepted 24 May 1995.